



JOINT 1D INVERSION OF MT AND TEM DATA FROM EBURRU, KENYA, AND PROCESSING OF GRAVITY DATA FROM THEISTAREYKIR, NE-ICELAND

Anna Wairimu Mwangi

Kenya Electricity generating Company

P.O. Box 785

Naivasha

KENYA

awmwangi@kengen.co.ke

ABSTRACT

The use of MT and TEM methods in geophysical exploration has been successful in studying geothermal fields. They have been used widely in Iceland and Kenya to investigate subsurface resistivity structures and to delineate the most favourable places to locate wells. In this report, electromagnetic methods, MT and TEM, are discussed and joint 1D inversion of MT and TEM data from the Eburru field in Kenya applied. In addition, the gravity method is briefly discussed, and data collection and processing applied to microgravity data from Theistareykir, NE-Iceland, for the purpose of monitoring mass depletion of the geothermal field prior to and during exploitation. The first part of the report discusses the resistivity methods and their application to Eburru and the second part the microgravity method and its application in Theistareykir. The MT and TEM data collected from Eburru are located around the prospect; they were processed and 1D inverted. The results are presented as 1D resistivity models for each individual sounding, as well as resistivity cross-sections and iso-resistivity maps. The TEM data were used to correct for the static shift of nearby MT soundings through joint 1D inversion. The results indicate a high resistivity at shallow depths caused by unaltered rocks. In some areas low resistivity appears close to the surface which is attributed to geothermal manifestations. A conductive cap is seen below the high resistivity, presumably corresponding to the smectite zeolite zone and reflecting an alteration temperature of 100-220°C. Below the conductive cap a resistive core is found, probably consisting of a mixed-layer clay zone and a chlorite-epidote zone reflecting an alteration temperature above 240°C. These temperature values might have decreased due to cooling. The resistivity reflects alteration, not necessarily the temperature. Still further down, a very low resistivity is found which probably indicates the heat source. The correlation between resistivity and temperature in the wells is discussed.

Data collection of microgravity data is discussed as well as the processing of the microgravity data. Emphasis, however, is laid on the field method, to ensure good quality data. The data are presented as reduced gravity values.

1. INTRODUCTION

The East African rift passes through Kenya (see Figure 1) which is the main reason why the country is vastly endowed with geothermal resources. The East African rift was formed by the process of continental rifting where two continental plates have been moving away from each other. The East African rift is though in principle, a failed arm of these continental rifting processes, an activity that started about 30 million years ago. Magmatic activity associated with the rifting where the continental crust is thinning is the source of the geothermal heat below. The rifting of the Kenya rift starts in Turkana and extends to the south towards Lake Magadi and still further into Tanzania. The molten rock is very close to the surface in the floor of the rift. Hence, it heats up the surrounding rock and the water flowing from the highland to the lower rift zone in the hydrological cycle is heated up and transported through convection to the surface as hot springs and geysers. Within the rift valley spectacular scenes of these geothermal manifestations are common.

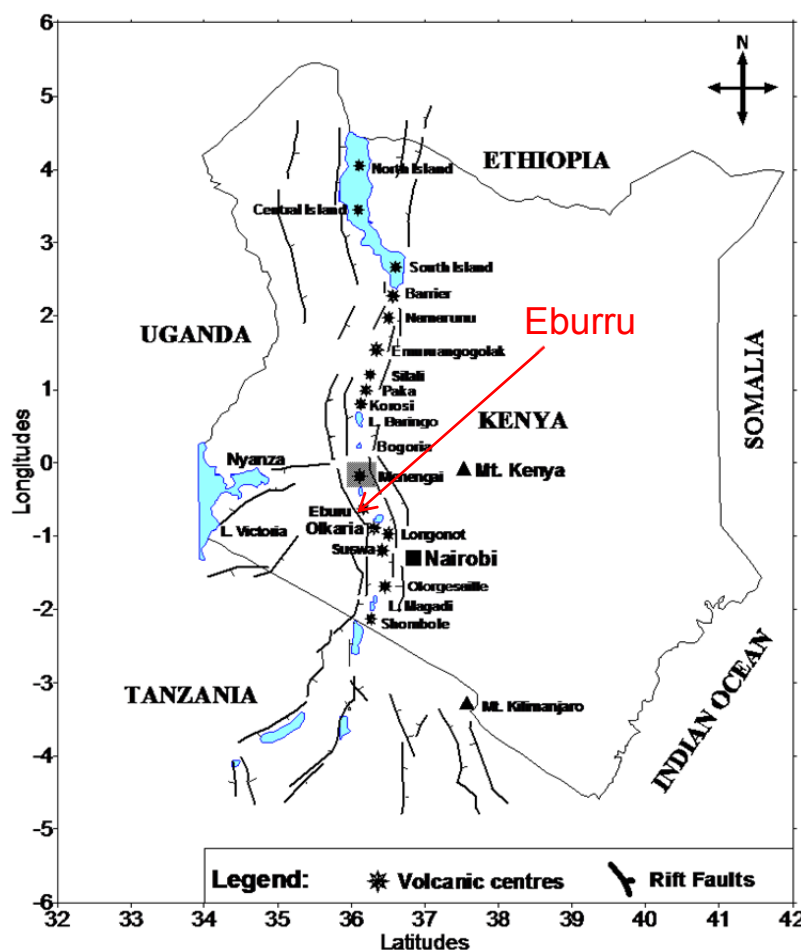


FIGURE 1: Location map of the East African rift passing through Kenya, and the Eburru geothermal field (modified from Ouma, 2010)

approximately 500,000 years old. The surfaces preserved on the youngest flows suggest that they erupted within the last 1,000 years (Velador et al., 2002).

In this report the results of the processing and joint 1D inversion of resistivity data, MT and TEM, from Eburru are shown as resistivity cross-sections and iso-resistivity maps. The models reveal the subsurface resistivity structure of Eburru and add further to the understanding of the geothermal system.

Eburru is one of the geothermal fields located south of the equator, about 20 km north of Olkaria geothermal field in Kenya (Figure 1). The Eburru volcanic complex is located in the Kenyan rift and is known to have the highest peak in the Rift valley with an elevation of about 2800 m. The field has been studied actively by KenGen since 1987. These studies led to the drilling of 6 exploration wells in the late eighties. This field is currently under development by KenGen for a 2.5 MW electrical power plant. The area has a population of about 100,000 people. Production of electrical power is very important for the development of the region. The Eburru field belongs to a complex of volcanoes – Menengai, Eburru, Olkaria, Longonot, and Suswa – that are centred on the Kenya Dome. All of these volcanoes are prime targets for exploitation and production of geothermal energy. Correlation with dated volcanism implies that the activity at Eburru is, at most,

The Theistareykir high-temperature geothermal area lies in an active zone of rifting and volcanism in northeast Iceland (Figure 2). It is within the Theistareykir fissure swarm. Iceland is an island that sits alone in the Atlantic Ocean on top of the Mid-Atlantic ridge. Due to active divergent plate movement, active volcanism is commonly witnessed along the active movement zones. This makes Iceland a place of vast geothermal resources due to the localized heat sources distributed along the rifting zones. Theistareykir was of important economic significance in earlier centuries as a source of sulphur which was exported by the King of Denmark (and Iceland) and utilized as a raw material for gun powder in Europe (Ármansson, 2009). Exploration of the area started in 1972; there is keen interest in monitoring this field. A microgravity survey was conducted in Theistareykir for the purpose of monitoring the future mass depletion in the area during the exploitation that is planned to begin in a couple of years. In this report, the gravity acquisition survey is discussed.

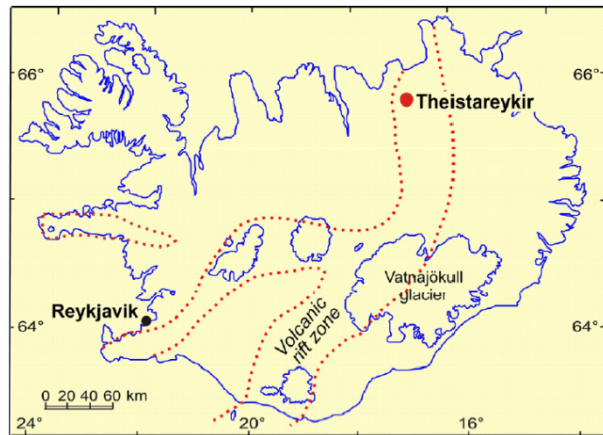


FIGURE 2: Map showing the location of the Theistareykir high-temperature field (red dot) on the western periphery of the Northern volcanic zone in Iceland

2. RESISTIVITY METHODS IN GEOTHERMAL EXPLORATION

2.1 Resistivity of rocks

Different rocks have different electrical resistivity. Taking an example of unaltered basalt, the resistivity is higher than 100 Ωm , while for basalts mineralized through geothermal activity it can be less than 10 Ωm (see Figure 3). This resistivity contrast makes it relatively easy to delineate resistivity anomalies caused by geothermal activity. The resistivity of rocks is predominantly dependent on a few factors. These properties determine the resistivity of rocks and, in particular, geothermal systems. These physical parameters are: temperature, porosity, permeability, salinity and hydrothermal alteration (Hersir and Björnsson, 1991). Electrical resistivity of rocks in geothermal surroundings is a parameter which reflects the properties of the geothermal system, or its history. Thus, a good knowledge about resistivity is very valuable for understanding a geothermal system. This relates to the fact that the resistivity of rocks is mainly controlled by parameters that correlate with geothermal activity, such as:

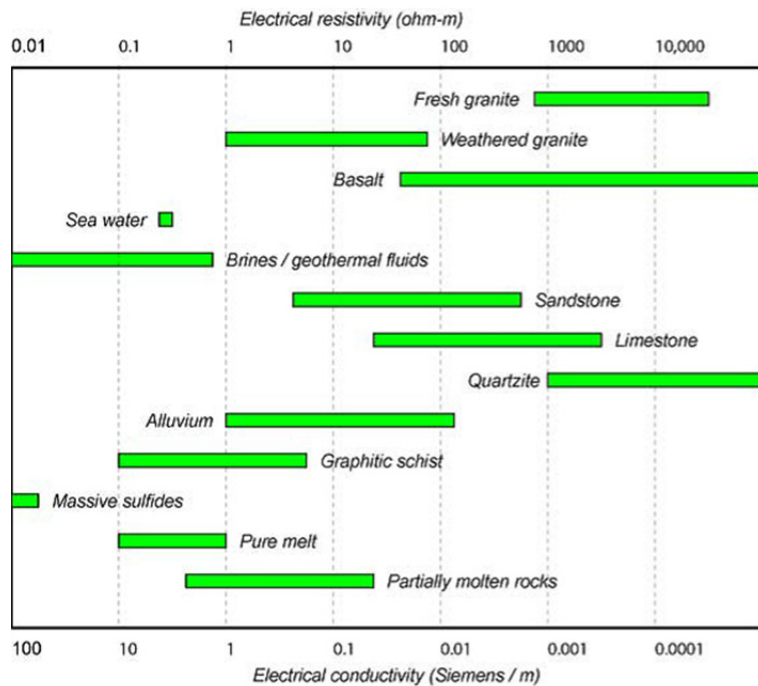


FIGURE 3: Electrical resistivity of different rocks in the earth's crust

- a) Porosity and pore structure, where a distinction is made between:
 - Intergranular porosity such as in sedimentary rocks;
 - Fracture porosity, relating to tension, fracturing or cooling of igneous rocks; and
 - Vugular porosity which relates to dissolving of material (limestone) or gas content (in volcanic magma);
- b) Alteration of the rocks lining the walls of the pores, often related to as water-rock interaction;
- c) Salinity of the fluid in the pores;
- d) Temperature;
- e) Amount of water, i.e. saturation or steam content

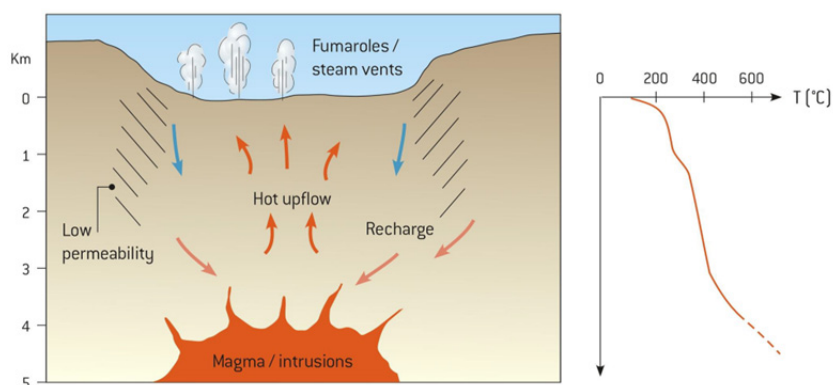


FIGURE 4: Geothermal system and the associated temperature gradient showing a heat source at depth where the recharge fluid comes into contact with conductively heated rock and a convective system of heated fluid which finds its way to the surface as hot springs and geysers (Axelsson, 2008)

The resistivity of rocks decreases when there is an increase in the fracture density of the rock, pore fluid, salinity and clay content and vice versa. The success of the application of the resistivity method for finding a geothermal system is attributed to the resistivity contrast of the alteration minerals associated with geothermal activity. The temperature gradient increases sharply with depth. Figure 4 shows a conceptual model for a geothermal system. The recharge area is

located at some distance through faults associated with rifting activity. The water comes into contact with the surrounding hot rock being heated below by hot magmatic intrusives. This causes hydrothermal fracturing of the surrounding rock, micro fractures and induced microseismicity. The fractures are the conduits for fluid flow. The heated water rises through convective movement to the surface while the cold fluid flows deeper and the process is repeated. The hot water interaction with rocks leads to desolution and deposition of minerals along these paths to the surface, dependent on the temperature at which each individual mineral precipitates (Axelsson, 2008).

2.2 Resistivity structure in high-temperature geothermal systems

Resistivity methods are commonly applied to delineate geothermal systems for the purpose of locating suitable sites for drilling. In most places in the world where the host rocks are volcanic, not sedimentary, they have a similar resistivity structure. They are characterized by some kind of a convex structure. At a certain depth, a low resistivity (conductive) cap or zone domes up (the outer margin of the reservoir) and is underlain by higher resistivity, a resistive core.

In high-temperature systems the interaction of water and rock, mostly referred to as the water rock interaction, combined with increasing temperatures causes dissolution, formation and deposition of minerals. The degree of hydrothermal alteration depends on the type of rock, chemistry of the geothermal fluids, permeability and porosity. The subsurface resistivity structure in high-temperature geothermal fields, therefore, reflects hydrothermal alteration. Figure 5 summarizes the alteration minerals produced at depth as a function of temperature and resistivity.

In the uppermost and unaltered part of the subsurface, resistivity is relatively high and the electrical conduction is mainly pore fluid conduction. The resistivity decreases within the conductive zone, as

the smectite-zeolite zone is reached, and mineral conduction becomes the dominant conduction mechanism. Resistivity decreases mainly because the ions in smectite and zeolites are loosely bound and, hence, they are free and can move and carry charges. Below, the mixed clay zone becomes dominant and the resistivity increases again within the resistive core, most likely due to the strongly reduced cation exchange capacity of the clay minerals in the mixed clay and the more deeply lying chlorite and epidote zone. The chlorite alteration starts at about 230°C and epidote begins at still higher temperatures around 250°C. These high-temperature and resistive minerals are strongly bound in the crystal lattices and, hence, are highly resistive. Not so many years ago most scientists found it hard to believe that resistivity would increase at this depth since the temperature obviously increases with depth (Hersir and Árnason, 2009).

If the alteration and temperature are in equilibrium, the subsurface resistivity structure reflects not only alteration but also which temperature to expect. This was an important finding, because if the temperature that produced the alteration mineralogy prevails, the resistivity structure can be used to predict the temperature.

But if cooling occurs, the alteration remains; in this case, the resistivity structure does not reflect the prevailing conditions but is more fossilized. This means it can only give an indication of the conditions prior to cooling. A good example is the Krafla geothermal field in NE-Iceland where the resistivity structure indicates that parts of the system are cooling (see Figure 6). However, there have been instances where alteration minerals indicated lower temperatures than those measured in the wells. When the alteration temperature is lower than the formation or the rock temperature, it can be inferred that the geothermal system is young, meaning it has not had enough time to form high-temperature alteration minerals. The young geothermal system is being heated up and alteration is lagging behind the formation temperature (Hersir and Árnason, 2009). In summary, we can conclude that measured resistivity reflects rock alteration and not necessarily the prevailing temperature conditions.

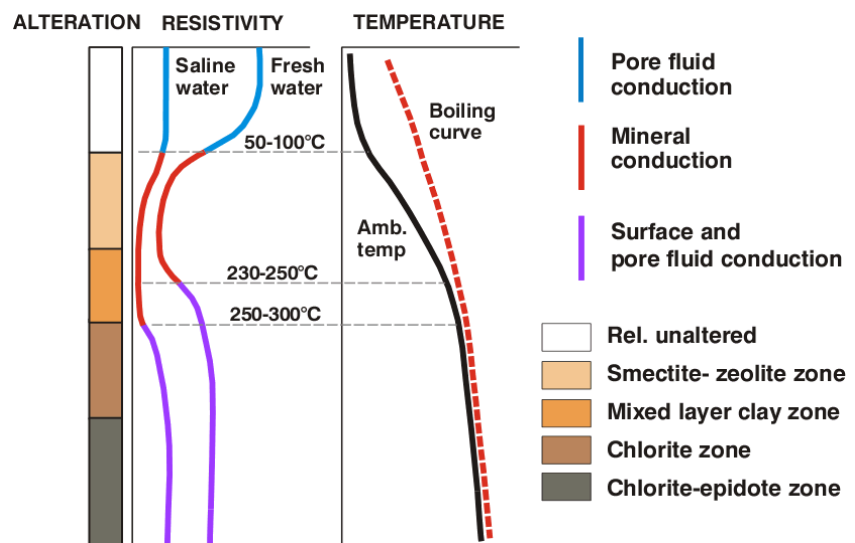


FIGURE 5: Summary of the relationship between Temperature gradient with depth, alteration, conduction mechanism and resistivity of rocks (Flóvenz et al., 2005)

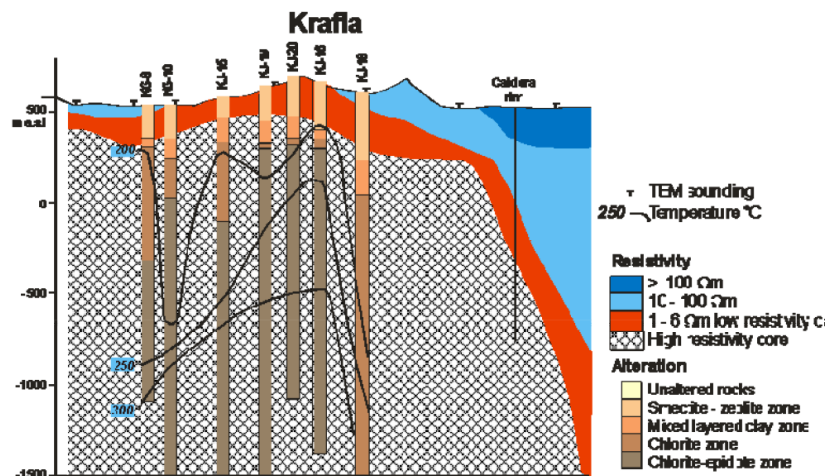


FIGURE 6: An example of cooling in a geothermal system – resistivity cross-section from Krafla geothermal field, NE-Iceland, showing alteration zoning and temperature (Árnason and Karlsdóttir, 1996)

3. RESISTIVITY METHODS

3.1 DC methods

DC resistivity methods have been used widely, especially before the advancement of electromagnetic methods, in the exploration of geothermal resources. DC measurements are the oldest of the resistivity methods, at least as methods used for geothermal exploration, and were the routine methods used in the 1950s-1980s, but their application is not as common nowadays. Most of the configurations rely on two pairs of electrodes— one pair for current transmission and the other pair for measuring the potential difference. The configuration defines the type. A distinction is made between a sounding and profiling. A sounding, which is much more common, has a fixed centre; varying the electrode spacing is used for mapping resistivity changes with depth. In profiling, the electrode distances are fixed, and the whole array is moved along the profile line for mapping lateral changes. The most common configurations, at least in geothermal exploration, are:

- *Schlumberger sounding*, which has been widely used for a long time and is still the most popular DC method. The electrodes are kept on a line, and the setup is mirrored around the centre. The pair of potential electrodes is kept close to the centre, while the pair of current electrodes is gradually moved away from the centre, for the current to probe deeper and deeper into the earth.
- *Dipole sounding or profiling*; here various arrays exist, many used quite extensively in the 1970s into the 1980s.
- *Head-on profiling*, a successful method for locating near-surface vertical fractures or faults. It is really a variation of the Schlumberger configuration with a third current electrode located far away at a right angle to the profile line.

3.2 Electromagnetic methods

Electromagnetic methods have been used extensively in the surface exploration of geothermal resources. They depend on the concept of time varying electric and magnetic fields that penetrate into the earth. Hence, when measured they give information on the subsurface resistivity structure. The way the electromagnetic waves diffuse into the earth is dependent on the resistivity structure of the earth below the measuring site.

3.2.1 TEM

Transient Electromagnetics (TEM) can be used to explore subsurface anomalies resulting from geothermal activities. In this report, the most important role for TEM is using it to correct for the static shift problem of the magnetotelluric method. Transient Electromagnetics have been used widely in geothermal exploration since the method gained popularity in the late 1980's. When compared with the Schlumberger soundings, this method is cheaper and more convenient in geothermal exploration since no current is injected into the ground. The method makes many areas, which are practically inaccessible to Schlumberger soundings, easily accessible for geothermal exploration, e.g. on glaciers (Árnason, 1989). One of the most important aspects of the TEM method is its application in correcting for the static shift of magnetotellurics. The TEM method, in addition, has the advantage that it is not sensitive to lateral variations as are DC methods (Árnason, 1989).

In the TEM method, current is transmitted into a large square loop often 200 m × 200 m in the survey area. A steady current is transmitted into the loop for a sufficiently long time to allow turn on transients in the ground to dissipate. The quiescent current is then sharply terminated in a controlled fashion. In accordance with Faraday's law, rapid reduction of the transmitter current, as well as of the transmitter primary magnetic field, induces an electromotive force (*emf*) in nearby conductors (see Figure 7). The magnitude of this *emf* is proportional to the time rate of change of the primary magnetic field at the

conductor. For this reason, it is desirable to reduce a large transmitter current to zero in a short time so as to achieve a large emf of short duration. This emf causes eddy currents to flow in the conductor with a characteristic decay which is a function of the conductivity, size, and shape of the conductor. The decaying currents generate a proportional (secondary) magnetic field and a time rate of change which is measured by a receiver coil placed in the centre of the transmitter loop (the configuration is called central loop TEM).

The setup of a central loop TEM sounding is shown in Figure 7. A current is transmitted in the loop and then sharply terminated. An induced current diffuses downwards and outwards and the inner loop (receiver coil) measures the response generated by the decaying magnetic field after the current is turned off.

An analysis of the nature of the transient decay is carried out by sampling the amplitude at numerous intervals of time, called gates. Moreover, this sampling is done over many cycles of the transmitter pulse so as to enhance the signal to noise ratio.

The output of the survey is an accurate knowledge of the three spatial components of the time derivative of the secondary magnetic field as a function of its position on the earth's surface; from this data much information can usually be derived about a survey target (MacNeill, 1980). The TEM configuration can be done in various setups, i.e. central loop TEM and GDC. In this report, the focus is on central loop TEM. In summary, current distribution and decay rate recorded as a function of time depend on the resistivity structure below the measuring site, and can be interpreted as such. The signal can also be based on a grounded dipole to create a primary magnetic field. TEM data are presented on a bi-logarithmic scale as DC data, but here the apparent resistivity is plotted as a function of time after the current was turned off.

The apparent resistivity is obtained after rigorous calculation and for the late times it is given by the equation below:

$$\rho_a(t) = \frac{\mu_o}{4\pi} \left\{ \frac{2\mu_o I_o A_r n_r A_s n_s}{5t^2 V(t, r)} \right\}^{\frac{2}{3}} \tag{1}$$

- where A_r = Cross-sectional area of the receiver coil (m^2);
- n_r = Number of windings in the receiver coil;
- μ_o = Magnetic permeability in vacuum (H/m);
- A_s = Cross-sectional area of the transmitter loop (m^2);
- n_s = Number of windings in the transmitter loop;
- $V(t)$ = Voltage as a function of time;

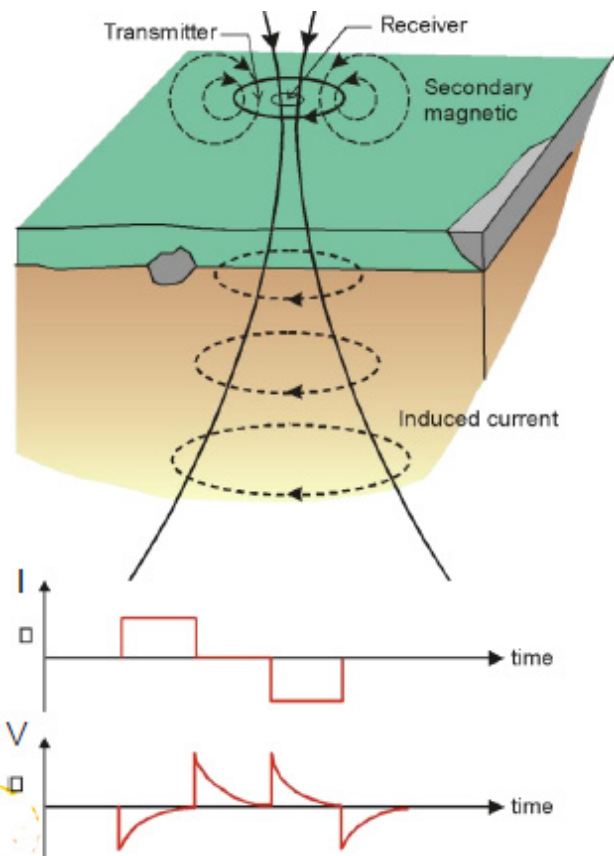


FIGURE 7: Layout of a TEM sounding, showing the current transmitted through the transmitter loop and the receiver coil in the inner loop that measures the response from the decaying magnetic field; the current is plotted as a function of time and voltage, showing the decay of the magnetic field (Hersir and Björnsson, 1991)

$\rho_a(t)$ = Apparent resistivity as a function of time; and
 t = Time elapsed, after the transmitter current was turned off.

3.2.2 MT method

The concept behind the MT method is that it utilizes the naturally occurring electromagnetic waves that are generated in the earth's atmosphere by a range of physical mechanisms. When these waves travel into the earth's interior, they decay at a rate depending on their frequencies. Low frequency signals travel further into the earth than high frequencies. The orthogonal electric (**E**) and magnetic (**H**) fields on the earth's surface are measured and, through Maxwell's relationships, the electrical resistivity models of the earth are inferred. Modern magnetotellurics consist of two interwoven branches: the magnetotelluric sounding, MT sounding, where the variations of the **E** and **H** fields are simultaneously measured; and the magnetovariational sounding, sometimes referred to as a geomagnetic depth sounding where only the **H** variation is measured (Berdichevsky and Dmitriev, 2008).

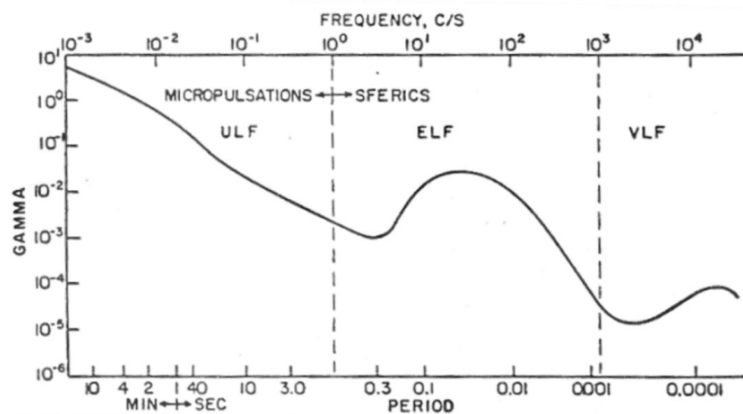


FIGURE 8: The MT “deadband” at 0.5-5 Hz at and the AMT “deadband” at 1-5 kHz

Audio magnetotellurics have the same concept as MT, the only difference being that higher frequencies in the range of 100-10,000 Hz are utilized. Distant lightning activity, the natural energy source for the audio-magnetotelluric (AMT) method, has a minimum signal between 1 and 5 kHz, the so-called AMT dead band (García and Jones, 2005). Similarly, the MT deadband is at 0.5-5 Hz (see Figure 8). The AMT signal is much stronger in the equatorial regions and reduces towards the polar regions.

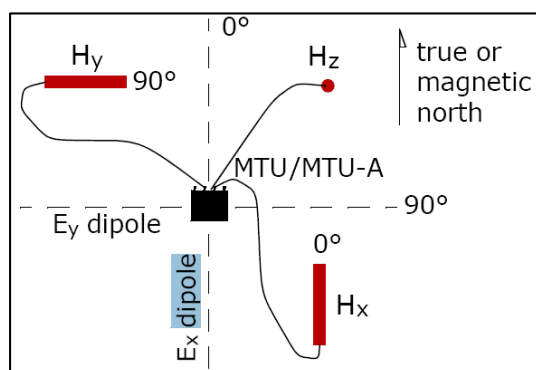


FIGURE 9: Layout of an MT sounding; the magnetic coils and the E dipoles are oriented orthogonally to each other with one of the magnetic coils vertical; the MTU/MTU-A is the acquisition unit (Phoenix Geophysics, 2005)

The MT equipment is portable and data collection is simple, involving measuring the magnetic field component **H** and the induced electrical field **E**, both as a function of time for several hours, at each site. MT measurements are, however, quite sensitive to cultural noise (power lines, houses, transformers, etc.). The MT layout is quite easy to do; the key thing to have in mind is to make sure the directions are accurately determined in order to collect reliable data. The MT layout is displayed in Figure 9.

The MT measurement probes a large volume of rocks and is therefore sensitive to 3D resistivity variations. Detailed interpretation can be difficult and may require 3D interpretation. More recently, the method has routinely been used in combination with TEM. The TEM measurements are used for mapping the uppermost kilometre in detail in order to enhance the

interpretation of the MT measurements, thus leading to better information at deeper levels. This way, good information on the distribution of the resistivity in the deeper parts of the geothermal system can be collected, reaching down to 5-10 km depth (Georgsson, 2009).

The main electromagnetic methods are Transient Electromagnetics (TEM), Magnetotellurics (MT) and audio magnetotellurics (AMT). These surface exploration methods have been used extensively in the oil and geothermal industries. They have been applied widely around the world with huge success and are relatively cheap and efficient ways for probing the subsurface. The electromagnetic methods are prone to cultural noise and need help to overcome this problem; sites for measurements should be selected away from sources of noise such as power lines. The concepts behind the method are expressed in differential form by the Maxwell's relationships:

$$\text{Faraday's law} \quad \nabla \times \mathbf{E} = -\frac{\partial \mathbf{B}}{\partial t} \quad (2)$$

$$\text{Ampère's law} \quad \nabla \times \mathbf{H} = \mathbf{J} + \frac{\partial \mathbf{D}}{\partial t} \quad (3)$$

$$\text{Gauss's law for electric field} \quad \nabla \times \mathbf{D} = \eta_V \quad (4)$$

$$\text{Gauss's law for magnetic field} \quad \nabla \times \mathbf{B} = 0 \quad (5)$$

where \mathbf{E} = Electrical field intensity (V/m);
 \mathbf{H} = Magnetic field intensity (T);
 \mathbf{J} = Electrical current intensity (A/m²),
 η_V = Electric charge density owing to free charges (C/m³);
 \mathbf{D} = Electric displacement current (C/m²)
 \mathbf{B} = Magnetic field (T)

Vectorial magnitudes in Maxwell's equations can be related through their constitutive relationships as shown below:

$$\mathbf{D} = \epsilon \mathbf{E}; \quad \mathbf{J} = \sigma \mathbf{E}; \quad \mathbf{B} = \mu \mathbf{H} \quad (6)$$

where ϵ = Electrical permittivity (C/Vm);
 σ = Electrical conductivity (S/m)
 μ = Magnetic permeability (H/m).

σ , ϵ and μ describe the intrinsic properties of the material through which the electromagnetic field propagates. These magnitudes are scalar quantities in isotropic media. In anisotropic materials, they must be expressed in a tensorial form (Castells, 2006).

The MT method is based on Maxwell's equations, aimed at obtaining useful information relative to the subsurface. The impedance tensor from Maxwell's relationship is used to derive the resistivity of the half space using the assumption that the earth below is homogeneous. In MT, the horizontal components of the \mathbf{E} field (E_x , E_y) are correlated with the horizontal components of the \mathbf{H} field (H_x , H_y) through the magnetotelluric impedance tensor.

$$Z_{xy} = \frac{E_x}{H_y} = \frac{i\omega\mu}{k} = \sqrt{i\omega\mu\rho} e^{i\pi/4} \quad (7)$$

$$Z_{yx} = \frac{E_y}{H_x} = -Z_{xy} \quad (8)$$

where \mathbf{Z} = Impedance tensor;
 $\pi/4$ = Phase difference between the electric and the magnetic field;
 Z_{xy} , Z_{yx} = Characteristic impedance in x and y directions;

- ω = Angular frequency ($2\pi f$) where f is frequency (Hz);
 μ = Magnetic permeability (H/m);
 $E_{x,y}$ = Electric field intensity (V/m) in x, y direction;
 $H_{x,y}$ = Magnetic field intensity (A/m) in x, y direction;
 k = $\sqrt{i\omega\mu(i\omega\varepsilon + \sigma)} \approx \sqrt{i\omega\mu\sigma}$ stands for the wave propagation constant.

The resistivity of a homogeneous half space is given as:

$$\rho = \frac{1}{\omega\mu} |Z_{xy}|^2 = \frac{1}{\omega\mu} |Z_{yx}|^2 \quad (9)$$

There are two apparent resistivity curves that are generated, i.e. the resistivity in the xy direction, ρ_{xy} and the resistivity in yx direction, ρ_{yx} . They are identical for a homogeneous half space.

The skin depth is defined as the depth where the electromagnetic wave has reduced to e^{-1} of its original value. It is expressed as:

$$\delta \approx 0.5 \sqrt{T\rho} \text{ (km)} \quad (10)$$

- where δ = Skin depth (km);
 T = Period (s); and
 ρ = Resistivity (Ωm).

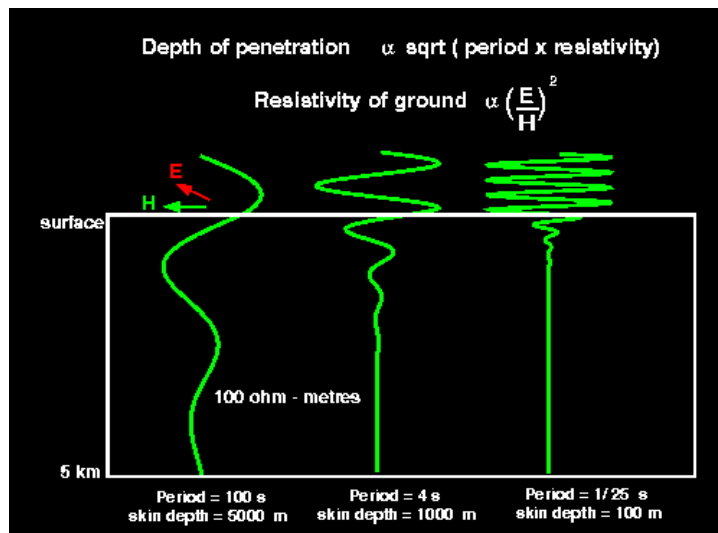


FIGURE 10: Display of the skin depth (depth of penetration) of the electromagnetic waves, depending on the frequency of the waves (University of Washington, 2011)

The magnetotelluric method probes deep and that is why it is referred to as a powerful method of exploration. It records low frequency waves which penetrate much deeper than the high frequency ones (see Figure 10). The skin depth can be of the order of tens of kilometres. The amount of time spent on recording the signal is one of the determinant factors on how deep into the earth's crust we can probe. The long period waves take a longer time to record. For deep crustal studies, the MT equipment is left to record for weeks but, for geothermal exploration, 24 hours is often enough to give sufficient information. It has an advantage over other electrical methods because it probes deep.

After data processing, the result is the MT impedance tensor as a function of frequency. It can be analysed to see which resistivity dimension of the earth it represents. In the analysis, the following is done:

1. Determining the *dimensionality* and *directionality* inherent within the MT impedance tensor, and their variations with frequency;
2. Derive response functions fully consistent with our assumptions about the earth (1D, 2D or 3D);
3. Determine whether MT tensor estimates are internally consistent;
4. Determine the extent of *static shifts*.

The general form of the impedance tensor is:

$$\begin{bmatrix} Z_{xx} & Z_{xy} \\ Z_{yx} & Z_{yy} \end{bmatrix}$$

For the 1D case, the diagonal elements of the impedance tensor, Z_{xx} and Z_{yy} are equal to zero, while the off diagonal elements are equal but have opposite signs. The tensor takes the general form of:

$$\begin{bmatrix} 0 & Z_{xy} \\ -Z_{yx} & 0 \end{bmatrix}$$

For the 2D case: In the electrical strike direction, the diagonal elements of the impedance tensor, Z_{xx} and Z_{yy} are equal to zero while for the off diagonal elements, $|Z_{xy}| \neq |Z_{yx}|$. This means that there are two apparent resistivities and they are not equal, i.e. $\rho_{xy} \neq \rho_{yx}$. The impedance tensor elements, Z_{xy} and Z_{yx} , are defined as the TE (**E**-polarization) mode and the TM (**B**-polarization) mode, respectively:

$$TE \text{ -mode:} \quad Z_{xy} = \frac{E'_x}{H'_y} = Z_{TE} \quad (11)$$

$$TM \text{ -mode:} \quad Z_{yx} = \frac{E'_y}{H'_x} = Z_{TM} \quad (12)$$

and $|Z_{xy}| \neq |Z_{yx}|$

Transverse electric (TE) mode is when **E** is parallel to the electrical strike direction and the transverse magnetic (TM) mode is when **E** is perpendicular to the strike.

3.3 Static shift

Magnetotelluric (MT) static shift is a non-inductive change of the MT apparent resistivity response that severely impairs the interpretation of data – a galvanic distortion. Static shift of the magnetotelluric apparent resistivity curve is caused by an erroneous measurement of the pertinent horizontal component of the earth's electric field of regional interest. The erroneous values are due to the potential differences between the electrode pair not truly representing the horizontal electric field component because of the presence of charges on local surface manifestations or near-surface, lateral inhomogeneities.

The effect is closely related to the current channelling problem of MT data (Jones, 1983); however, it differs from the latter in that even at the highest frequency, the potential difference does not give the correct amplitude for the regional electric field, whereas the phase lead of the electric field over the magnetic field is correct. However, a sufficiently short period's modelled apparent resistivity must asymptotically approach the correct value and, accordingly, these modelling studies illustrate current channelling rather than static shift. The basic difference between current channelling and static shift is that static shift does not affect the phases of the MT impedance tensor, whereas current channelling does. Thus, static shift is, as implied, a shift of the apparent resistivity curve by the same multiplicative factor at all frequencies such that the shape of the curve is retained when plotted on a log-ordinate scale without any corresponding change in the phase curve (Jones, 1988). Usually, TEM is used to correct for the static shift as it is not affected by static shift, using jointly inverted MT and TEM data.

Other attempts to solve the static shift problem are based normally on spatial filtering or some assumptions about the statistical distribution of the shift multipliers. One such is assuming that the product of all the multipliers for many soundings covering a big area is close to one. For this report, the spatial distribution map of the shift factor is used for the MT soundings that are not near a TEM sounding. Failure to correct for static shift will give wrong results and misleading interpretations of the resistivity model.

4. MT AND TEM SURVEY AT EBURRU HIGH-TEMPERATURE FIELD IN KENYA

4.1 Introduction

Significant geoscientific work was done at Eburru high-temperature geothermal field in Kenya in the 1980's; this culminated in the drilling of 6 exploration wells between 1987 and 1990. The wells drilled are EW-01, EW-02, EW-03, EW-04, EW-05, and EW-06. Their average depth is 2.5 km.

Geophysical methods, such as gravity and Schlumberger resistivity surveys, were carried out during the early stages of exploration. More recent work was done in 2006 and 2009, like MT, AMT and TEM electrical surveys. In this report, data obtained from MT and TEM during these surveys were processed and analysed. Of the exploratory wells drilled in this area, only EW-01, EW-04 and EW-06 were thermally productive, producing 2.4 MWe, 1.0 MWe and 2.9 MWt, respectively. The other wells, EW-02, EW-03 and EW-05, recorded maximum temperatures of 131, 161 and 156°C, respectively. Discharge fluid chemistry from the wells indicates that the reservoir is non-boiling with high-salinity brine and a high amount of non-condensable gases (NCG). Despite the almost similar geology, the chloride level of EW-01 (956 to 1976 ppm) is higher than the Olkaria average. As compared to Olkaria, the reservoir permeability is moderate (Lagat, 2003). Both the Olkaria and Eburru geothermal systems are volcano hosted resources and, thus, the heat driving the systems is associated with hot intrusive bodies under the volcanoes. The surface is covered with pyroclastics and lithological loggings indicated trachytes as the reservoir hosts. The heat source in the Eburru volcanic complex is probably from a localized intrusive of syenitic composition (Omenda and Karingithi,

1993). The area is characterised by craters and a ring structure but, just like Olkaria, it does not have a defined caldera. Figure 11 shows the geology of the area and Figure 12 a geological cross-section.

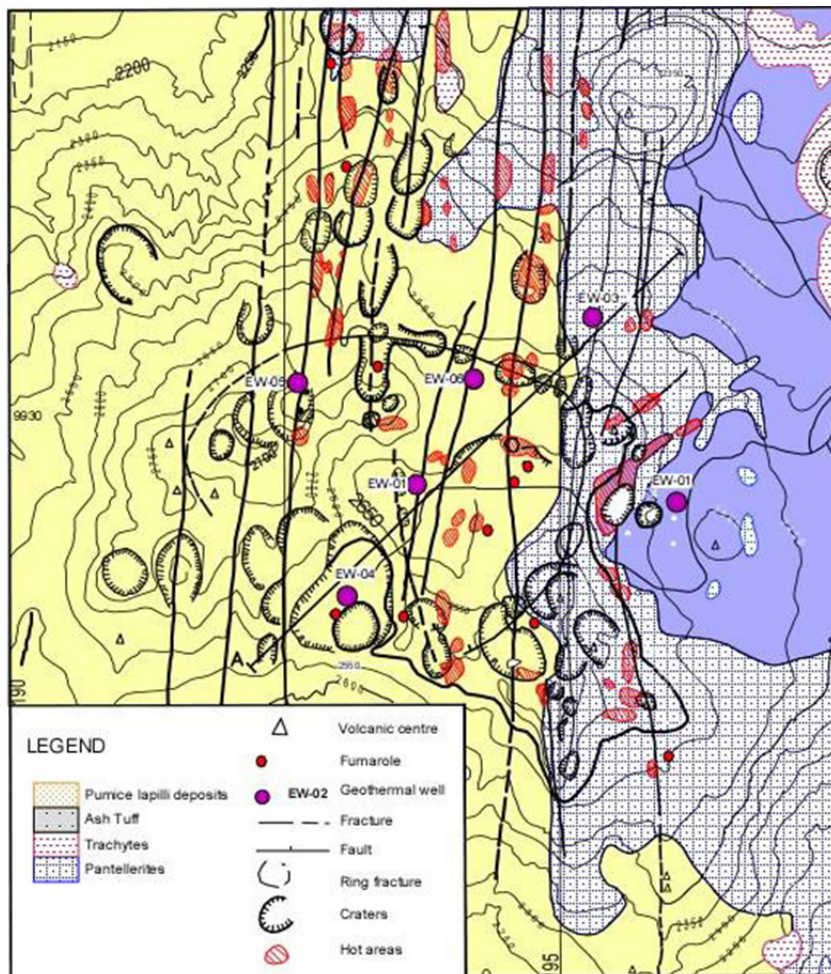


FIGURE 11: A geological map of Eburru showing the main structures of the prospect (Omenda and Karingithi, 1993)

Mapping indicates that the volcanic field is divided into an older western section, composed of pantellerites (Er1), overlying faulted trachytes (Et1), and a younger eastern section. The eastern section has a mappable ring structure, and is composed of trachytes (Et2) and pantellerites (Er2). Some of these flows may be contemporaneous, but the final phase of eruption is exclusively pantellerite. We have chemical data for all units except the older pantellerites. The data indicate that the trachytes and rhyolites are both pantelleritic in terms of their alumina and iron contents. This is in contradistinction to the

rhyolites immediately adjacent at Olkaria, which are comenditic. Concentrations for all elements are highly elevated, except for Ba, Sr, K, P, and Ti which show deep negative anomalies. The relationship between the trachytes (Et2) and pantellerites (Er2) is one in which the pantellerites consistently have the highest concentrations of all elements, including those with negative anomalies.

4.2 TEM, MT and AMT surveys

In all, 14 TEM soundings, covering an area of about 30 km², were carried out in Eburru geothermal field using the central loop TEM array (Figure 7). The equipment used for this survey was the Zonge system GDP-32 receiver. The current was transmitted using a 300 m × 300 m square loop, and the transmitter frequencies were 16 and 4 Hz. The TEM data were processed and used for static shift correction of the MT data. The Eburru TEM data were processed using TemX software were done (Árnason, 2006a) and the 1D interpretation was done using TEMTD software (Árnason, 2006b). The results of the individual soundings are presented in Appendix I in a special report including all the appendices to this report (Mwangi, 2011).

MT and AMT methods were applied to the Eburru field in two phases, the first phase in 2006 and the second phase in 2009. The data are distributed over an area of about 56 km² (see Figure 13). The data were collected using equipment supplied by Phoenix Geophysics, Canada. A total of 34 MT/AMT soundings were processed and analysed using the TEMTD program. The TEM data were used to correct for the static shift of the MT data. The static shift multipliers distribution was plotted and used to determine the shift multiplier for MT soundings without TEM, in a vicinity of less than 300 m.

4.2.1 Processing of TEM data

The TEM data were processed using the TemX program (Árnason, 2006a). The TemX software is written in ANSI-C and uses the XForms library (free software available on the web) for interactive graphics. The program comes in two versions: TemX which reads and processes central loop TEM data recorded by a PROTEM receiver from GEONICS; and TemxZ which reads and processes central loop TEM data recorded by a GDP-32 receiver from Zonge Engineering & Research Organization. The two versions only differ by the routines that read the raw data, but the data processing and

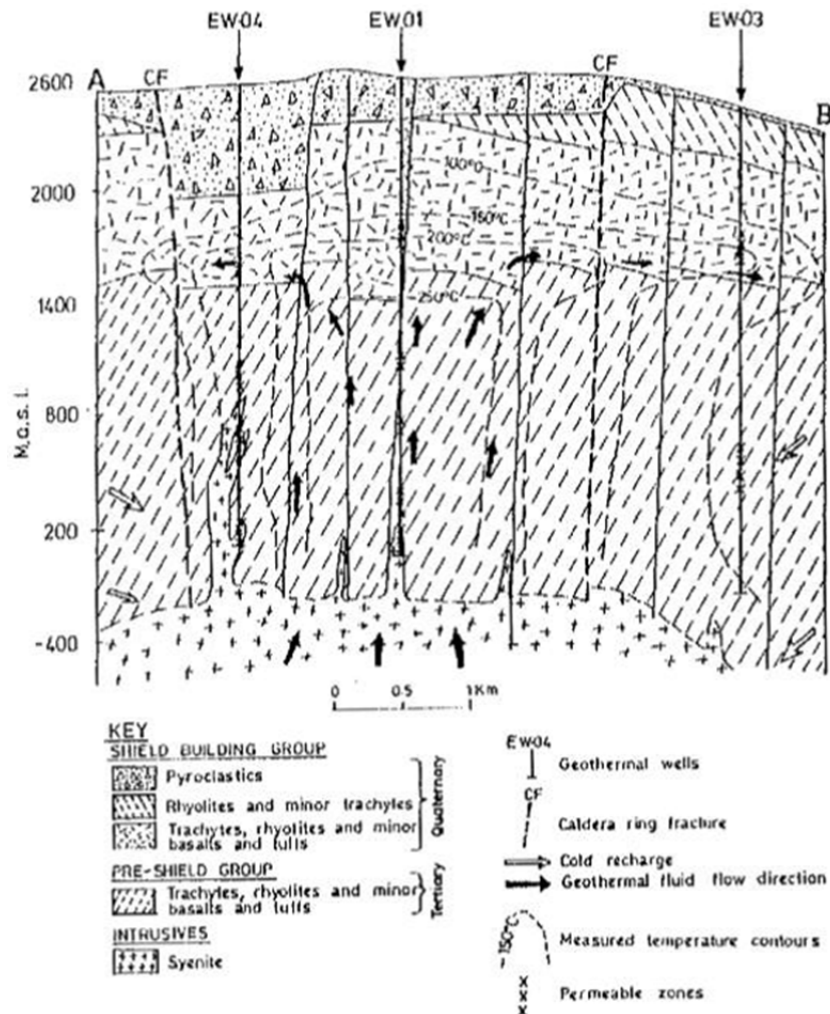


FIGURE 12: A geological cross-section of Eburru geothermal prospect, the location of the profile is shown in Figure 11 (Lagat, 2003; Omenda and Karingithi, 1993)

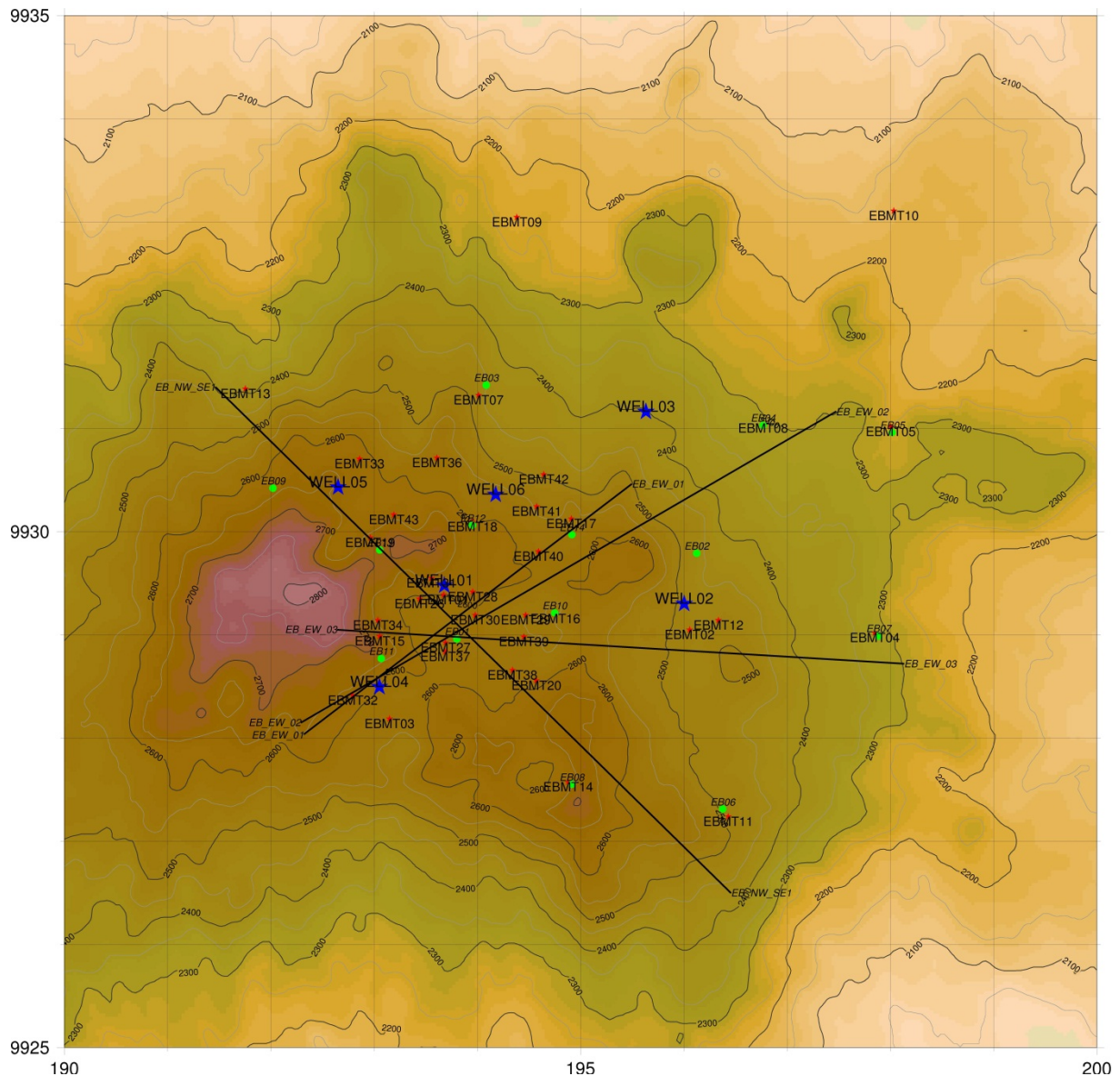


FIGURE 13: Location of MT soundings (red dots), TEM soundings (green dots) and the well locations (blue stars)

interface are identical. The TemX software reads files with datasets from a sounding. It performs normalization of the voltages with respect to the transmitted current, gain and effective area of the antenna and then displays all the data graphically, allowing the user to omit outliers, calculate averages over datasets and calculate late time apparent resistivity (Árnason, 2006a).

The TEM data are then inverted, using layered models as well as the Occam inversion, with the output looking like the sounding shown in Figure 14. All of the TEM soundings data and their associated 1D models are presented in Appendix I (Mwangi, 2011). The layered model is used as an initial model for the Occam inversion. Occam inversion of the layers is fixed; we only invert for the resistivity. The model is controlled such that we do not get sharp changes in the resistivity structure, unlike in the layered model where no constraint is put on the change in resistivity between layers.

4.2.2 Processing of MT data

The MT data were processed using SSMT2000 software from Phoenix Geophysics (2005), part of the processing software that is supplied with the MT equipment. The time series data were Fourier transformed then processed and edited in the MTEditor program. In this program, data are edited or

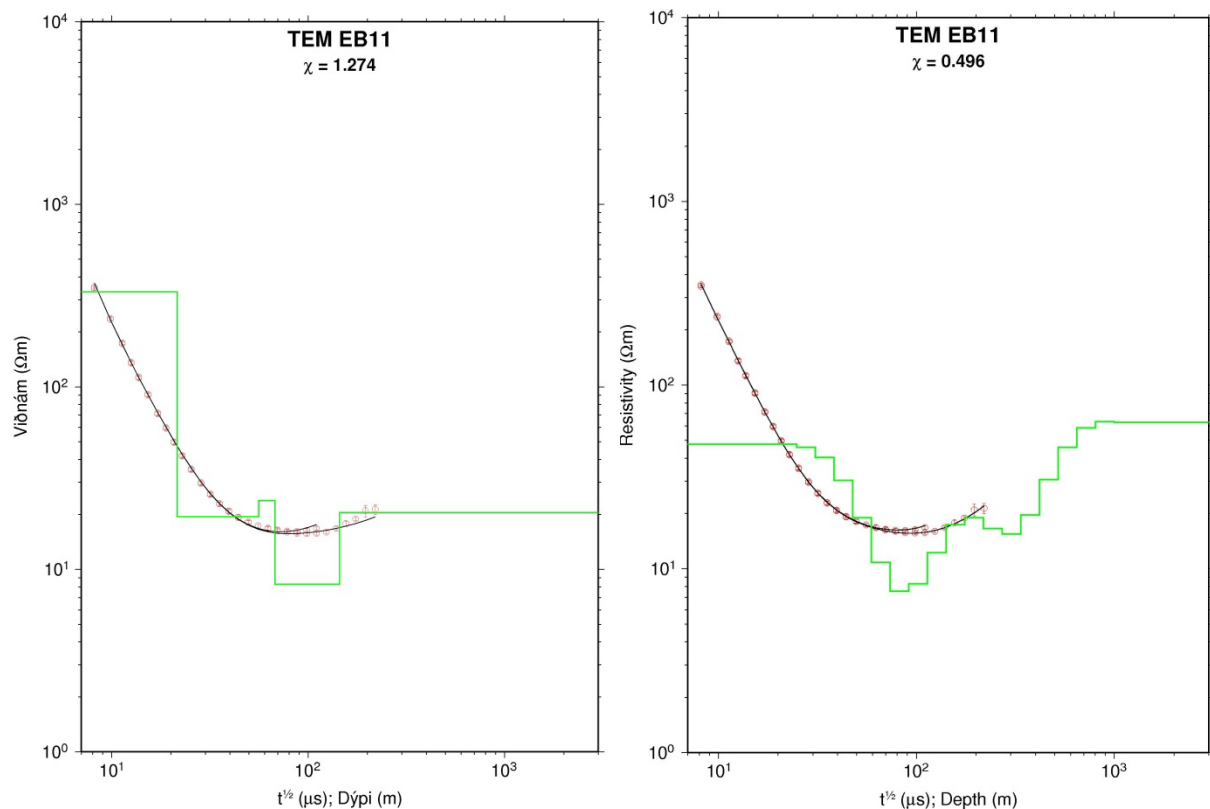


FIGURE 14: TEM sounding EB11 and its interpretation based on inversion, on the left based on a layered model but on the right Occam inversion: red circles: measured late-time apparent resistivities; black line: apparent resistivity calculated from the model, shown in green

sort of cleaned (removal of outliers) and at the end converted to EDI files. EDI stands for Electrical Data Interchange standard, which is an approved data format for MT data (SEG, 1991). The files created by SSMT2000 are used as input for the program which then displays the resistivity and phase curves as well as the individual cross powers that were used to calculate each point on the curves. Cross powers that were greatly affected by noise can be automatically or manually excluded from the calculations (see Figure 15).

The program allows the display of a variety of parameters of the plot files such as tipper magnitude, coherency between channels, and strike direction. The output is industry-standard EDI files suitable for use with geophysical interpretation software. There are two apparent resistivities, ρ_{xy} and ρ_{yx} . These are the blue and red curves, respectively, in the left top panel in Figure 15. The rotationally invariant determinant of the apparent resistivity and phase are used for inversion. The Zstrike shows the dimensionality of the subsurface resistivity. Figure 16 gives an example of processed data of an MT sounding. The processed data for all the MT soundings are given in Appendix II (Mwangi, 2011). For each site, the following MT parameters are shown, as seen in Figure 16:

- *Apparent resistivity* for both main modes (ρ_{xy} and ρ_{yx}) calculated in the measured directions, i.e. x is magnetic north and the y axis is magnetic east. Black circles denote the apparent resistivity derived from the rotationally invariant determinant of the impedance tensor.
- *Apparent phase* (θ_{xy} and θ_{yx}) calculated in the measured directions. Black circles denote the apparent phase derived from the rotationally invariant determinant of the impedance tensor.

Zstrike or the *Swift angle* gives the electrical strike, (the horizontal rotation which maximizes $|Z_{xy} + Z_{yx}|$), for each frequency and is shown by filled circles. The direction used for calculating apparent

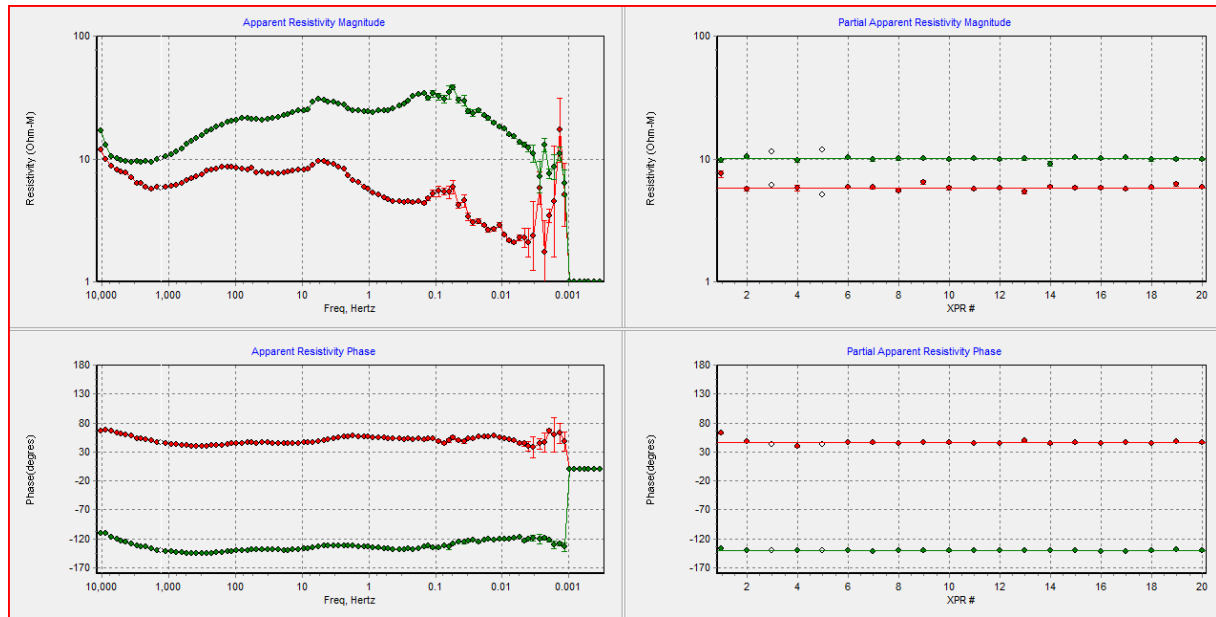


FIGURE 15: An example showing the plot of the apparent resistivity and phase (both the xy (red) and (yx) (blue)) vs. frequency for MT sounding EBMT40; outliers on the right hand window have been removed (not filled circles) to smooth the curves. The low-frequency part of the curve is usually noisy and often has to be cut off

resistivity and phase is shown by unfilled circles. For a two-dimensional electrical structure, a constant value of electrical strike would be observed.

1. Three dimensional indicators:

$$\text{Skew} = \frac{|Z_{xx} + Z_{yy}|}{|Z_{xy} - Z_{yx}|}$$

Swift skew is shown by black filled circles. It is rotationally invariant and should be zero for a 1D and 2D earth.

$$\text{SkewB} = \frac{\sqrt{|\text{Im}(Z_{xx}Z_{yy}^* + Z_{xx}Z_{yy}^*)|}}{|Z_{xy} - Z_{yx}|}$$

SkewB or *Bahr skew* is shown by unfilled circles. It is rotationally invariant and should be close to zero for both a 1D and 2D earth,

$$\text{Ellip} = \frac{|Z'_{xx} - Z'_{yy}|}{|Z'_{xy} + Z'_{yx}|}$$

Ellipticity is shown by grey dots. It is calculated using the principle rotational coordinates and gives the axis rotation of the electrical field's ellipse. A value of zero for both skew and ellipticity is a necessary and sufficient condition for two-dimensionality of the data.

The Coher shows the multiple coherency of the electrical fields with respect to the horizontal magnetic fields, in the measuring coordinates. The coherency is defined between 0 and 1. The higher the coherency is, the better are the data (preferably higher than 0.9) (Gylfi Páll Hersir, pers. comm.).

EBMT40

Skrá: EBMT40.EDI

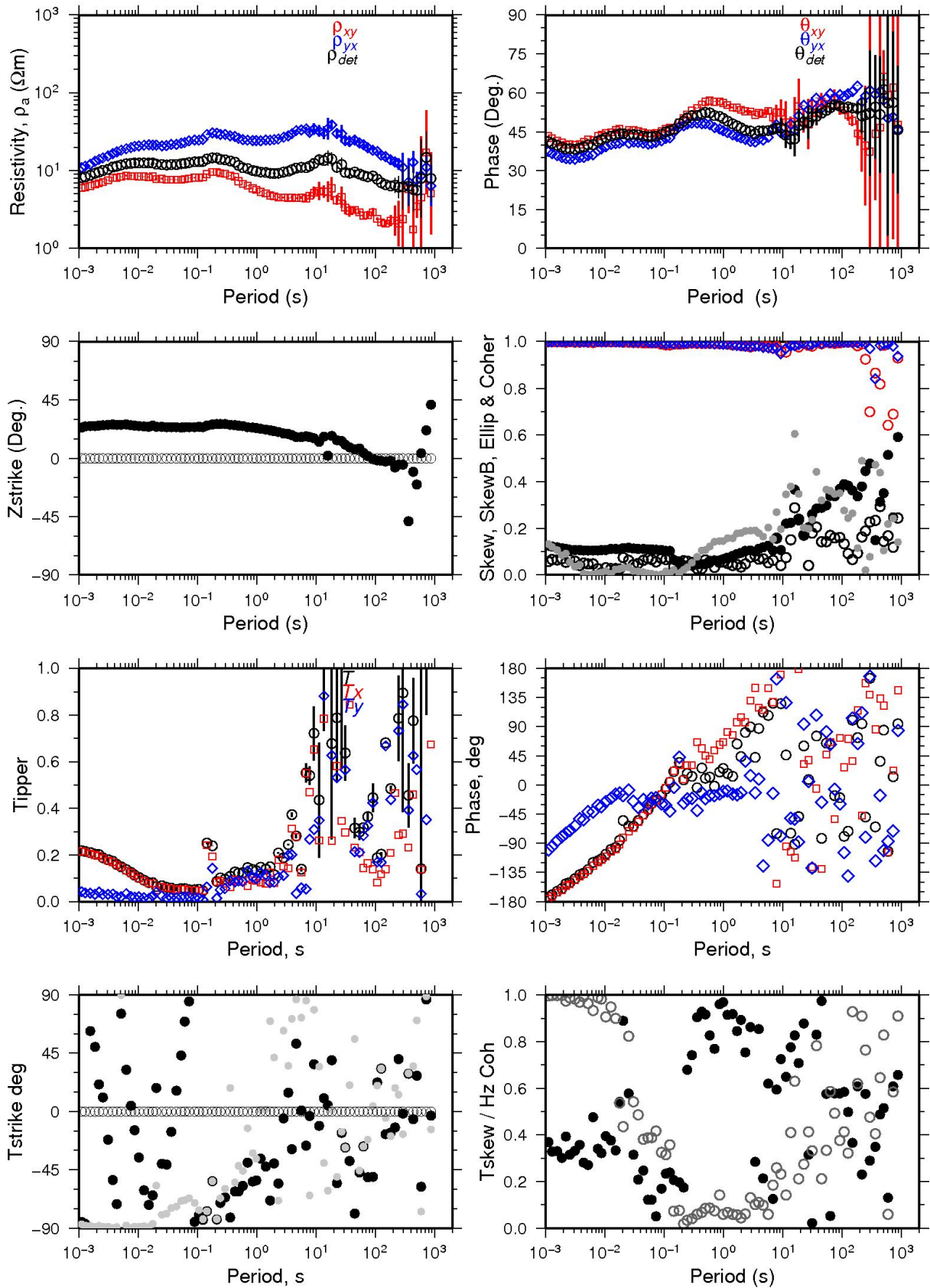


FIGURE 16: Example of processed data for MT sounding EBMT40

4.3 Joint inversion of TEM and MT data

A total number of 3 cross-sections were made to display the result of the 1D inversion of the MT and TEM soundings. The programme TEMTD performs 1D inversion with horizontally layered earth models of central loop transient electromagnetic (TEM) and magnetotelluric data and Occam (minimum structure) inversion. It can be used to invert only TEM or MT data and also for joint inversion of TEM and MT data, in which case it determines the best static shift parameter for the MT data. The current wave form is assumed to be a half-duty bipolar semi-square wave (equal current-on and current-off segments), with exponential current turn-on and linear current turn-off. For MT data, the programme assumes standard EDI for the impedance and/or apparent resistivity and phase data. The programme is written in ANSI-C and runs under UNIX/LINUX operating systems. It uses the gnuplot graphics programme for graphical display during the inversion process (Árnason, 2006b). Soundings once prepared are jointly inverted. This is important because it not only solves the problem of static shift in MT but also helps resolve the uppermost layers close to the surface because TEM is mainly 1D and, therefore, gives accurate 1D information on the earth directly below. The TEM data are jointly inverted, generating a model which is presented on a logarithmic scale as resistivity vs. depth (Figure 17). The program allows performing iterations in order to obtain the best fit of the TEM and MT curves. The shift factor is determined and it is printed in the plots with values usually ranging from 0.1 to 2. A value of 1 means that the MT curve is not shifted and does not suffer static shift.

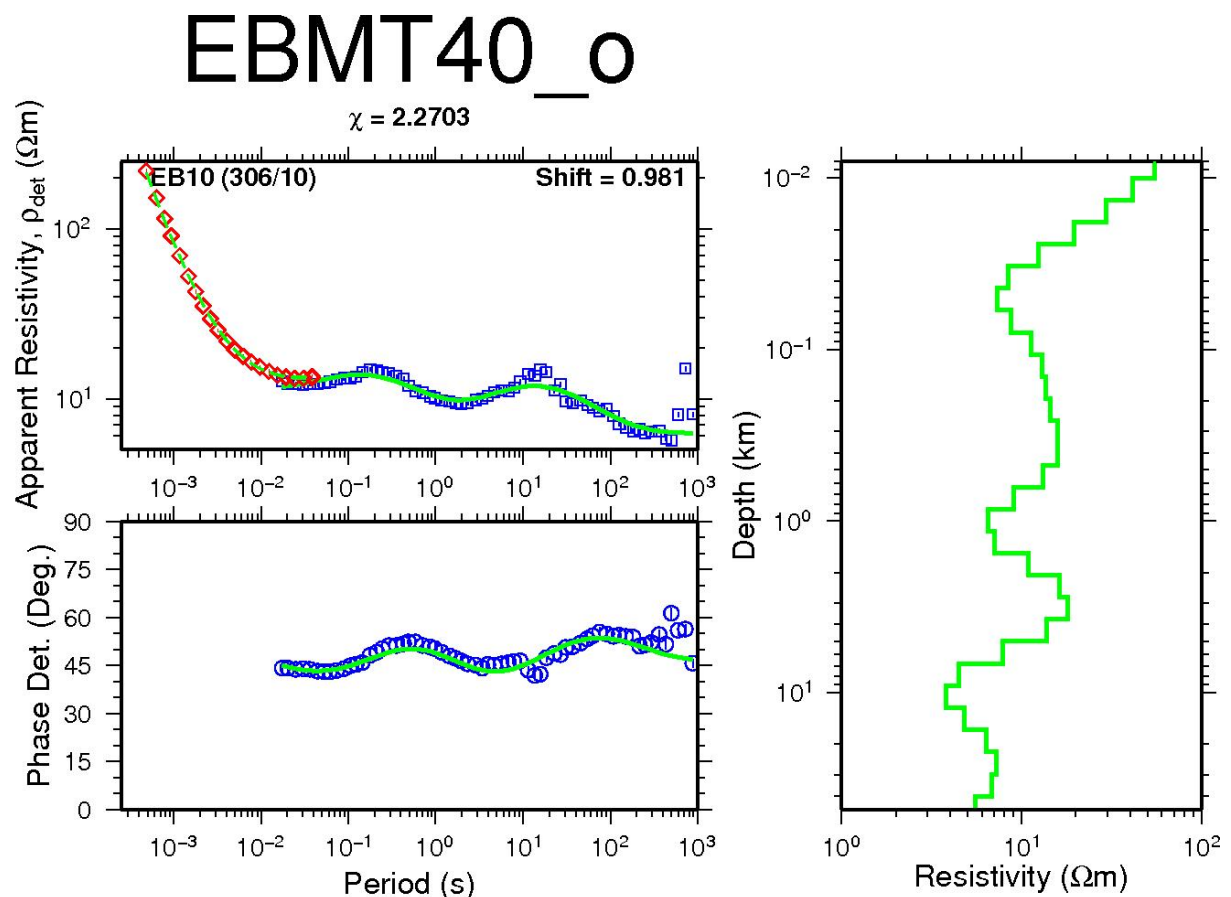


FIGURE 17: Joint 1D inversion of TEM and MT data: red diamonds: measured TEM apparent resistivities; blue squares: measured apparent resistivities; blue circles: apparent phase derived from the determinant of MT impedance tensor; green lines: on the right show the results of the 1D resistivity inversion model; to the left is synthetic MT apparent resistivity and phase response. The number on the top of the figure, EBMT40, corresponds to the name of the MT station and the bold number in the resistivity panel, EB10, is the name of the TEM station. The numbers in parentheses (306/10) mean that the two stations were 306 m apart and their elevation difference was 10 m. Chi square χ is the misfit

Values as low as 0.1 mean that the shift factor is high and the shift was great. The plots also show the distance between the TEM and the MT soundings as well as the difference in elevation. Chi square χ , is the misfit. The final plots give depth vs. resistivity models. These are later used to make cross-sections and iso-resistivity maps to illustrate the 1D model of an area.

TEM/D allows performing inversion of MT data alone. The soundings that were inverted alone were MT soundings that did not have a nearby TEM station. Therefore, a static shift map was made to estimate the shift factors to be used when inverting the MT soundings. The map assisted in correcting for the static shift of MT but did not successfully do the proper correction. It should be emphasized that MT cannot be corrected by itself and needs a TEM station within a radius of 100-200 m. Figure 18 shows the static shift map made for Eburru. The 1D joint inversion models for all the TEM and MT pairs is given in Appendix III (Mwangi, 2011). The static shift map made for Eburru is shown in Figure 18 and the histogram of the static shift parameters in Figure 19. The static shift parameters range from 0.2 to 1.2. The histogram indicates that about 50% of the MT determinants were shifted downwards whereas 20% did not show any static shift and 30% shifted upwards. The estimation of

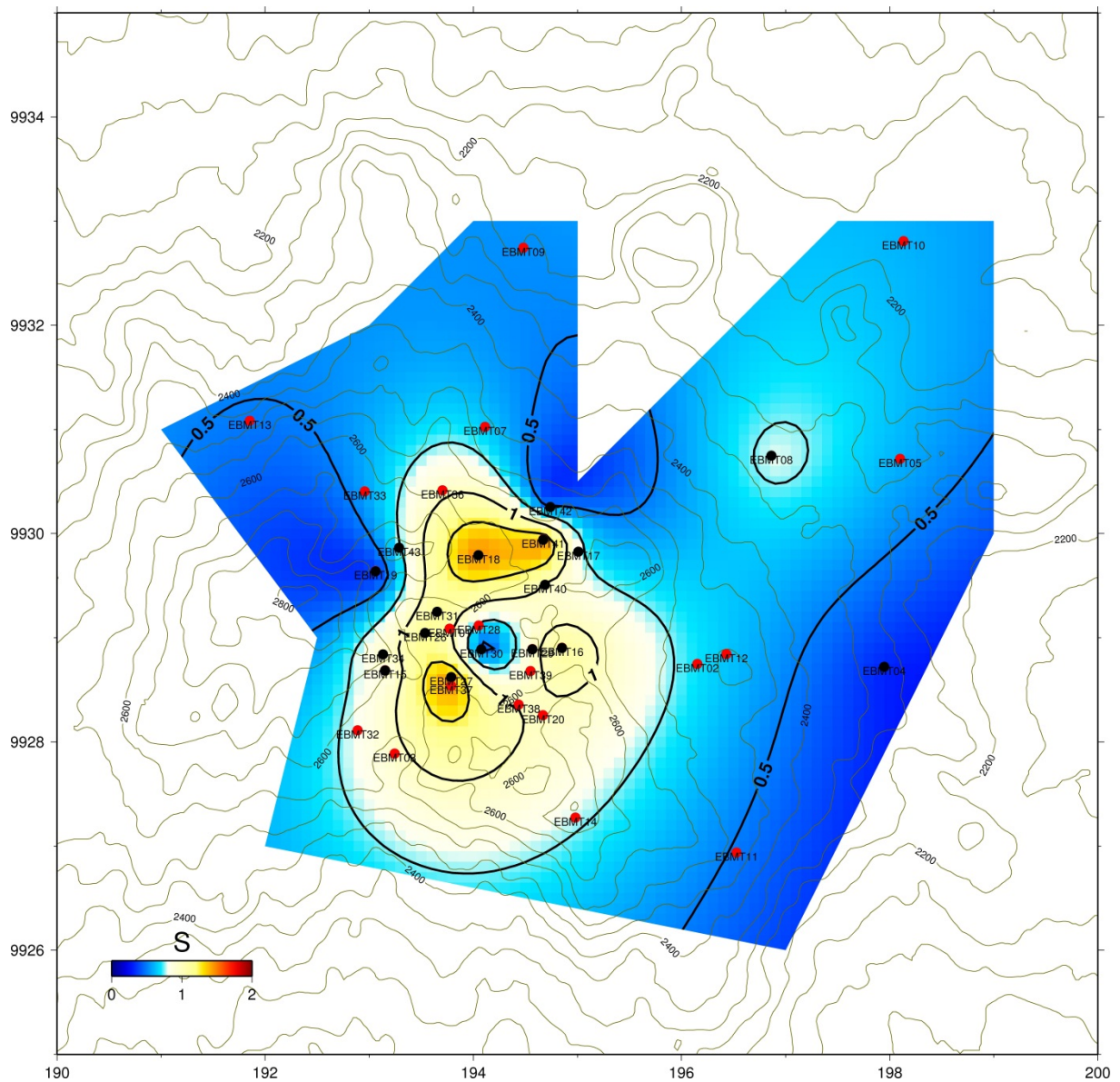


FIGURE 18: Spatial distribution of static shift parameters in Eburru geothermal field. Black dots denote sites where joint inversion was performed and red dots denote sites where joint inversion was not performed due to the lack of a nearby TEM sounding

the static shift is an attempt to solve the shift in MT but it can lead to errors in resolving the resistivity structure. The best way to correct for the shift is to carry out TEM measurements in the vicinity of the MT to remove the shift in MT, using the uppermost resistivity values determined by the TEM.

4.4 Cross-sections

To represent the resistivity structure of Eburru, resistivity cross-sections of the 1D inversion data were compiled to evaluate how the resistivity changes with depth.

Profile EB_EW_02. Figure 20 shows resistivity variations along profile EB_EW_02. At shallow depth, the resistivity is high, caused by unaltered rocks. At some places at the surface there is very low resistivity which is interpreted as sites having geothermal manifestations such as fumaroles which are abundant in the area. Below about 1500 m a.s.l., a

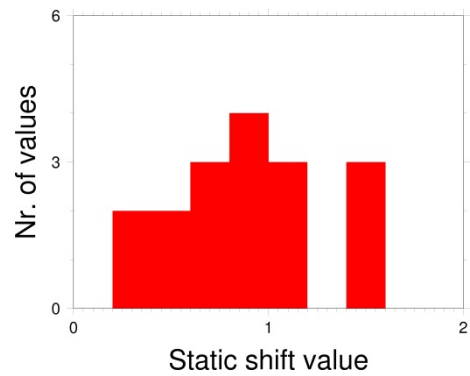


FIGURE 19: Histogram of static shift parameters in Eburru

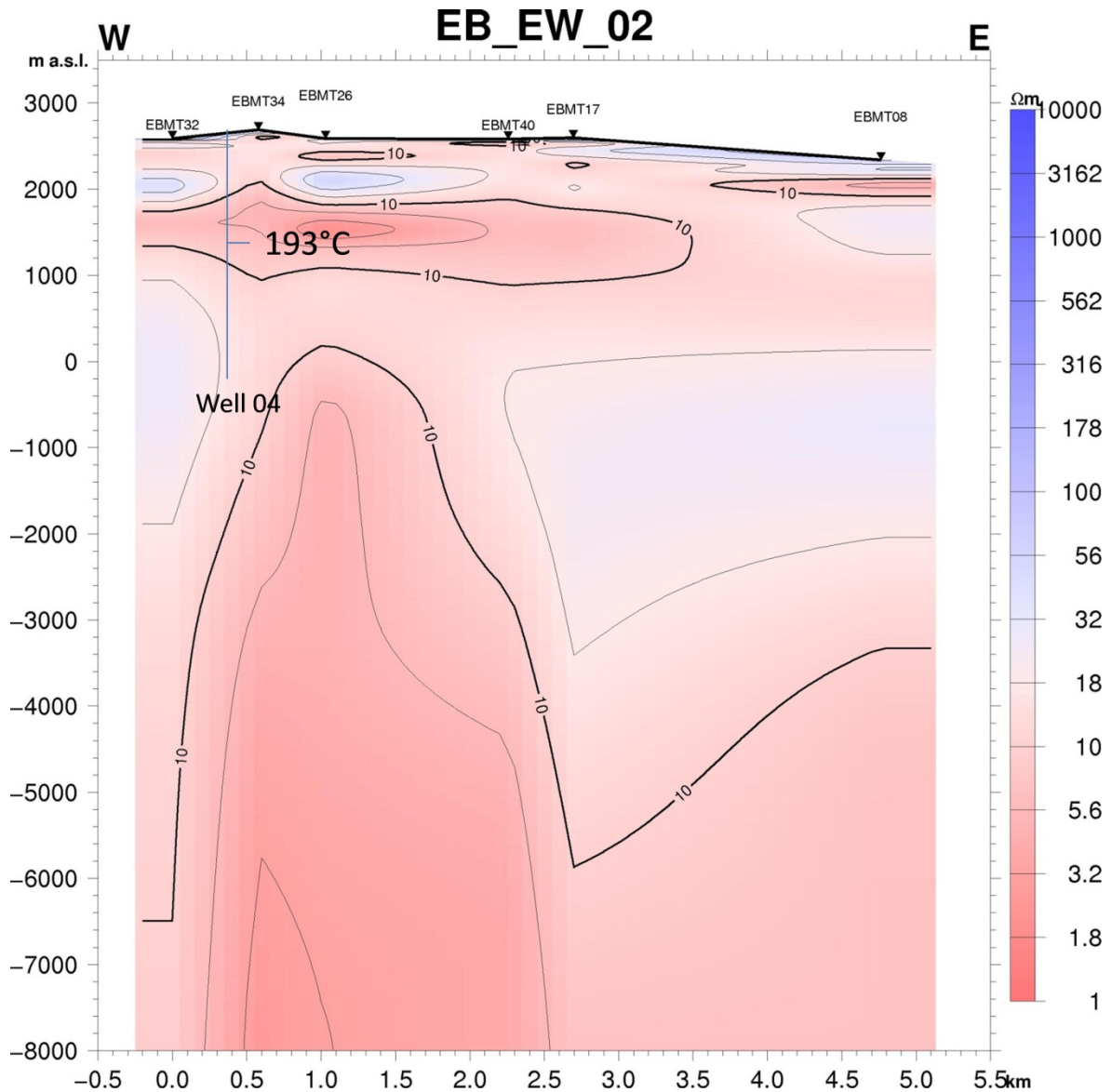


FIGURE 20: Resistivity cross-section EB_EW_02 down to a depth of 8000 m b.s.l.; the location of the profile is shown in Figure 13

conductive cap is seen and is interpreted as the smectite zeolite zone. At about 1000 m a.s.l., high resistivity is found, presumably indicating the mixed-layer clay zone; further below is the epidote-chlorite zone. The lowest layer seen is a conductive layer which persists to the depth of 8000 m b.s.l. The top of this layer is at sea level and it is interpreted as the heat source. The Eburru area hosts intrusive bodies and this could be a hot intrusive body which acts as the heat source. Well 01, with recorded temperatures above 270°C, seems to be right on top of this zone (see Figure 21).

Profile *EB_EW_01* (Figure 21) shows similar resistivity structures as profile *EB_EW_02*. The profile has a larger conductive surface, attributed to alteration at the surface. The conductive cap - the smectite-zeolite zone, is seen at a depth of 2100 m a.s.l. and is well delineated. It is somewhat thinned. Underlying this, a resistive zone is seen which forms a layer and persists to a depth of more

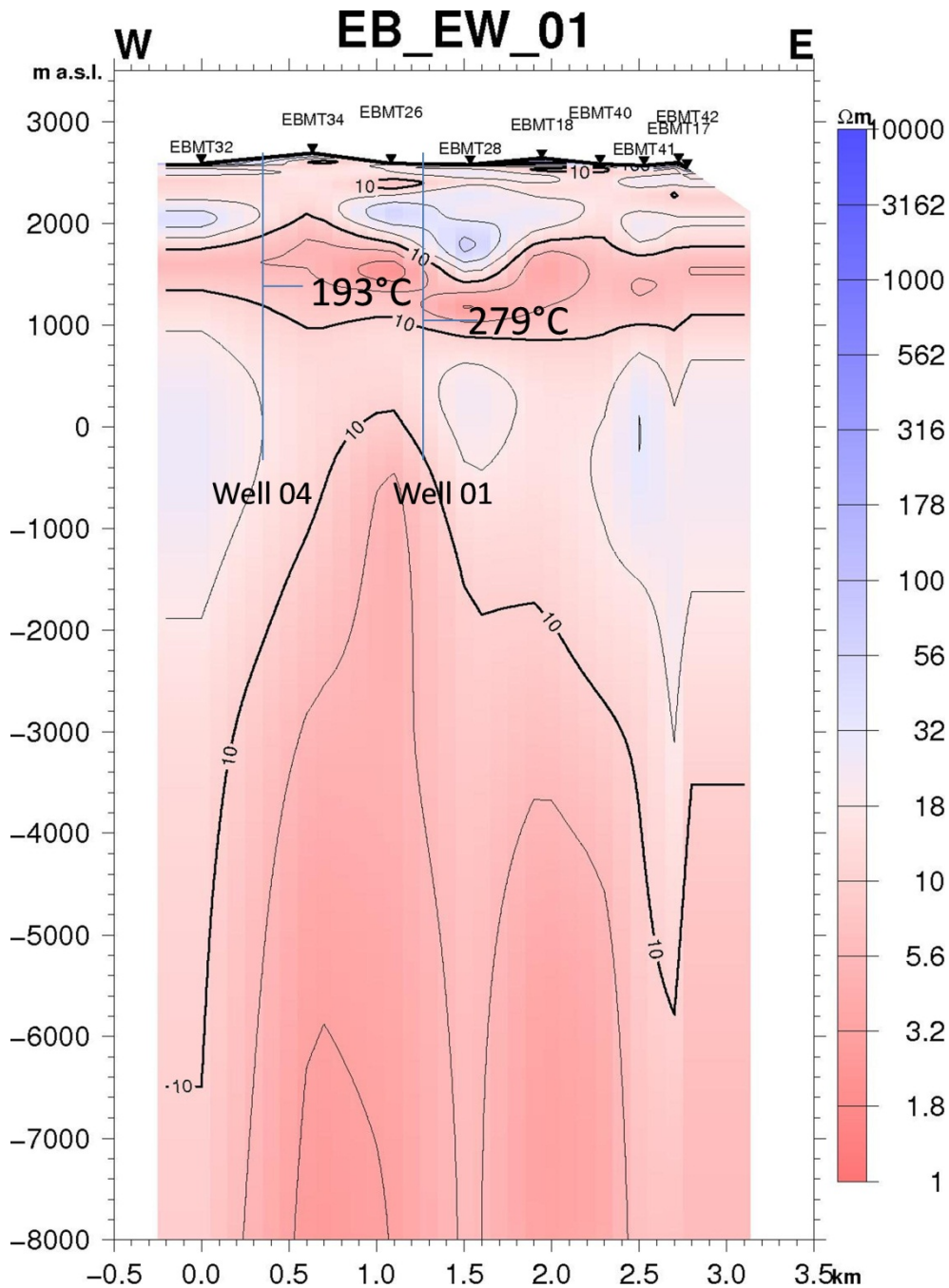


FIGURE 21: Resistivity cross-section EB_EW_01 down to a depth of 8000 m b.s.l.; the location of the profile is shown in Figure 13

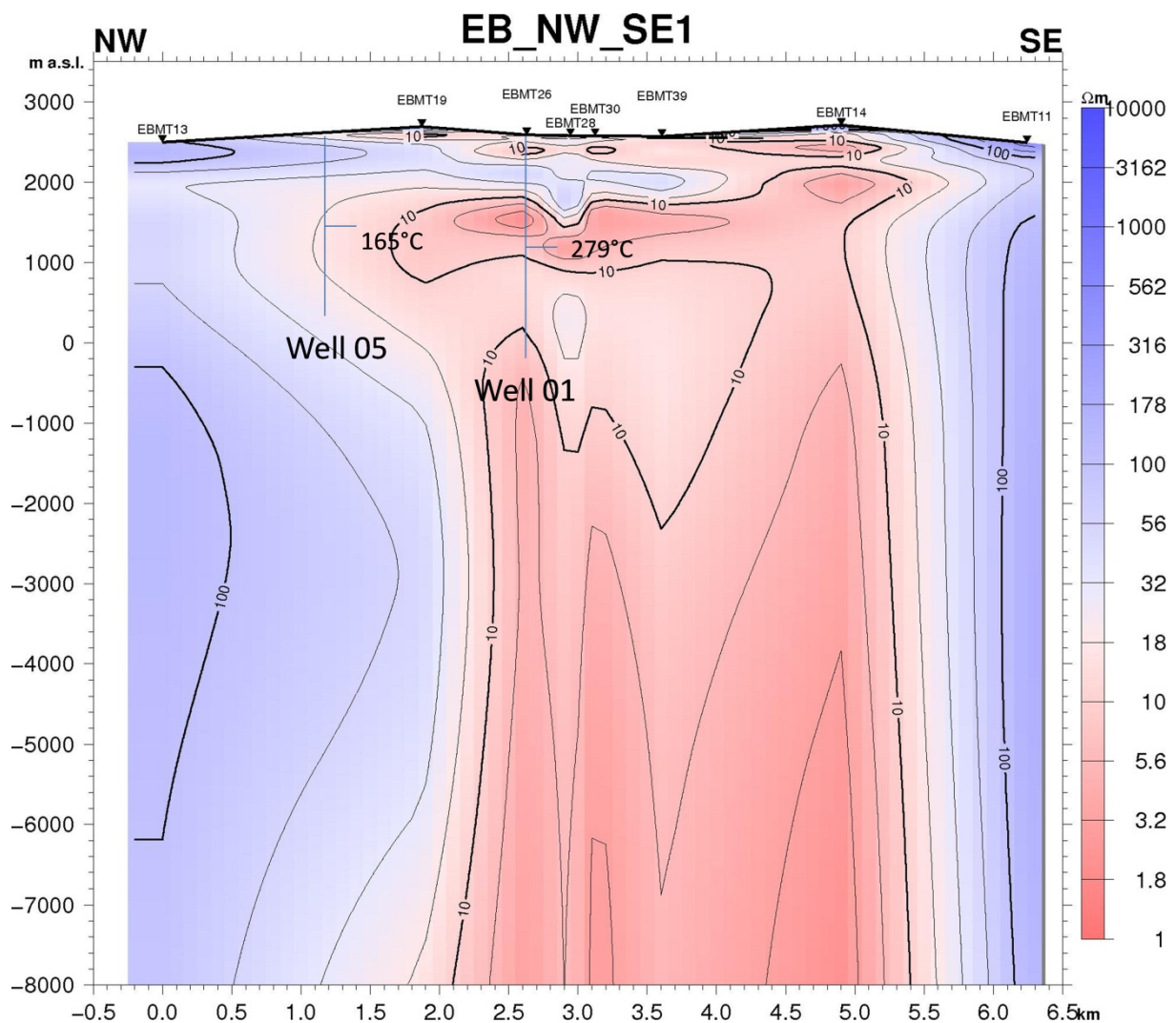


FIGURE 22: Resistivity cross-section EB_NW_SW_01 down to a depth of 8000 m b.s.l.; the location of the profile is shown in Figure 13

than 2000 m. This is interpreted as the chlorite-epidote zone which overlies a conductive structure which extends to the bottom of the cross-section, at a depth of 8000 m b.s.l. This section compliments Figure 20. The resistivity decreases with depth below sea level. The structure seems like an intrusive heat source at sea level. Figure 22 shows *cross-section EB_NW_SW01* which reveals similar structures as in the previous sections.

4.5 Iso-resistivity maps

The iso-resistivity maps show resistivity variations at a certain depth. They are drawn at depths which show the most interesting variations. Here, four maps are presented, at 1500 m a.s.l., at sea level and 3000, and 6000 m b.s.l. (Figures 23-26). The iso resistivity maps also display the location of the wells. The iso-resistivity map in Figure 23 reveals the extent of the conductive cap with resistivity $<10 \Omega\text{m}$, indicating the conductive smectite-zeolite clay zone. Wells EW-04 and EW-01 tap from this zone and their temperatures are 193 and 279°C, respectively (see also Figure 20). The resistivity starts to increase again close to sea level (Figure 24). This is attributed to the formation of the high-temperature minerals chlorite and epidote, which are resistive minerals. The resistivity then decreases again, as seen at the deeper levels of 3000 and 6000 m b.s.l. (Figures 25 and 26). Additional iso-resistivity maps and a cross-section are given in Appendices IV and V (Mwangi, 2011).

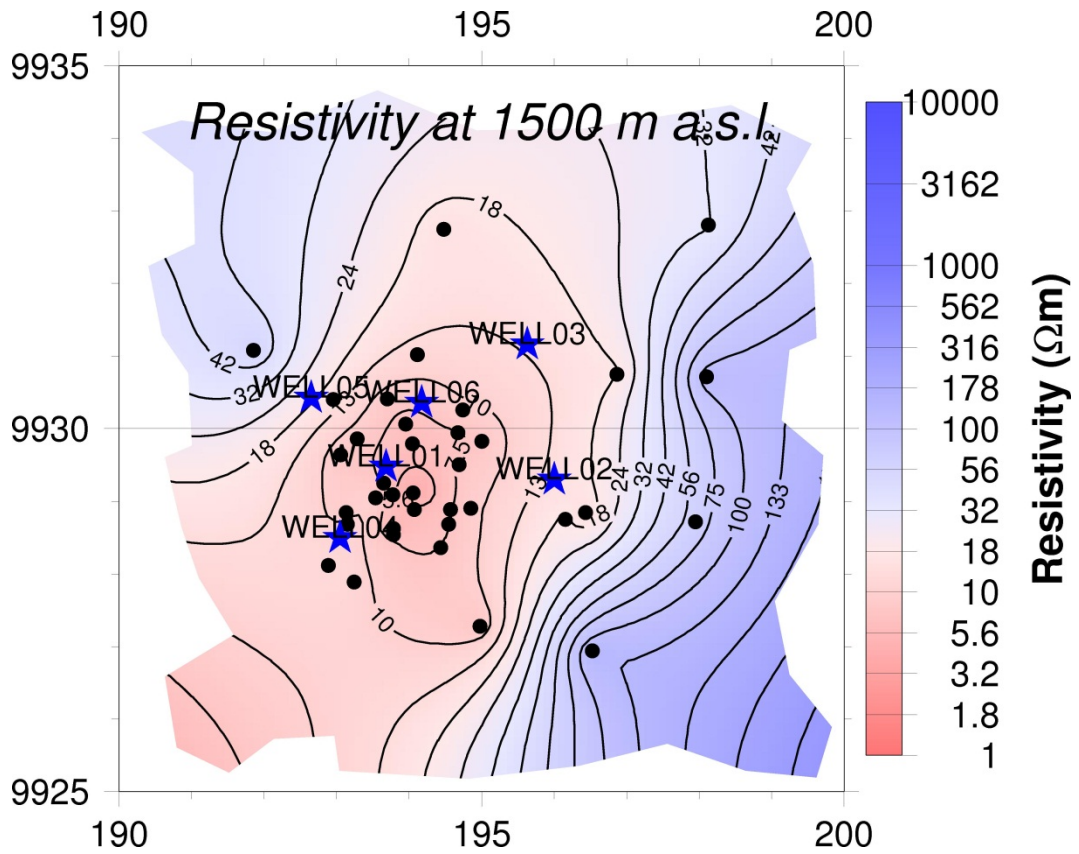


FIGURE 23: Iso-resistivity map at a depth of 1500 m a.s.l.; black dots denote MT soundings; blue stars show wells

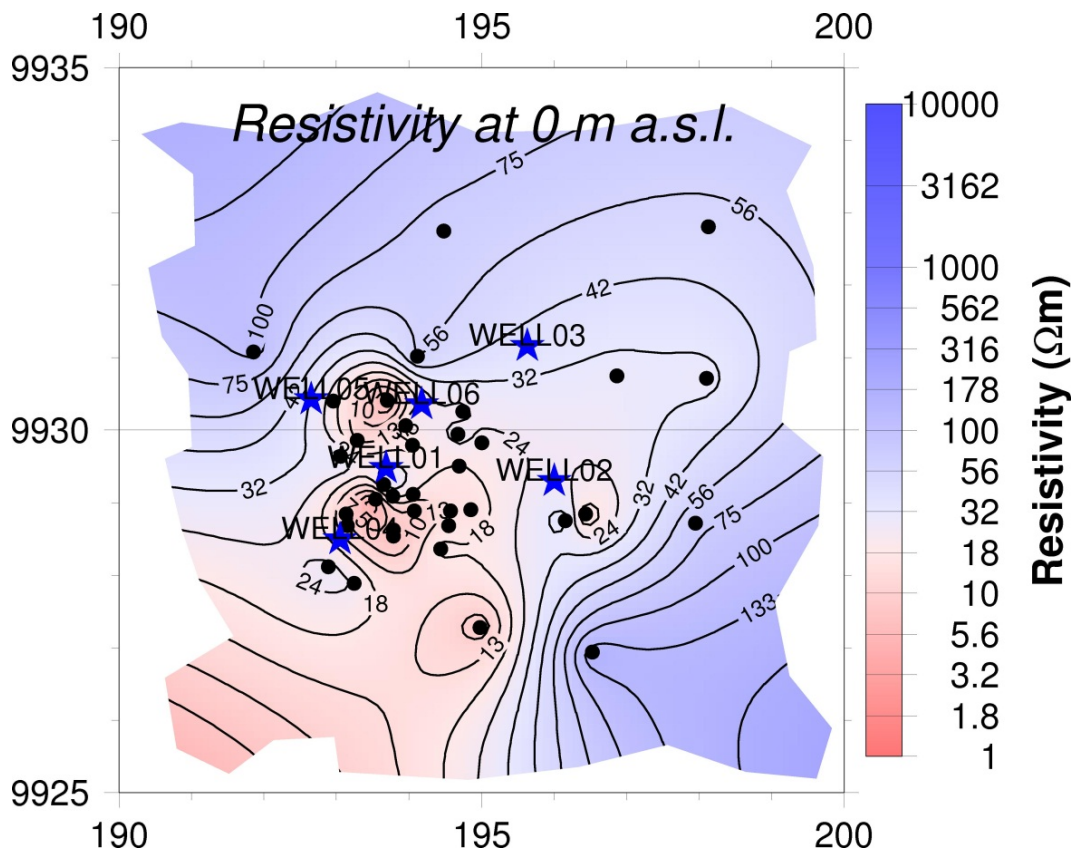


FIGURE 24: Iso-resistivity map at sea level

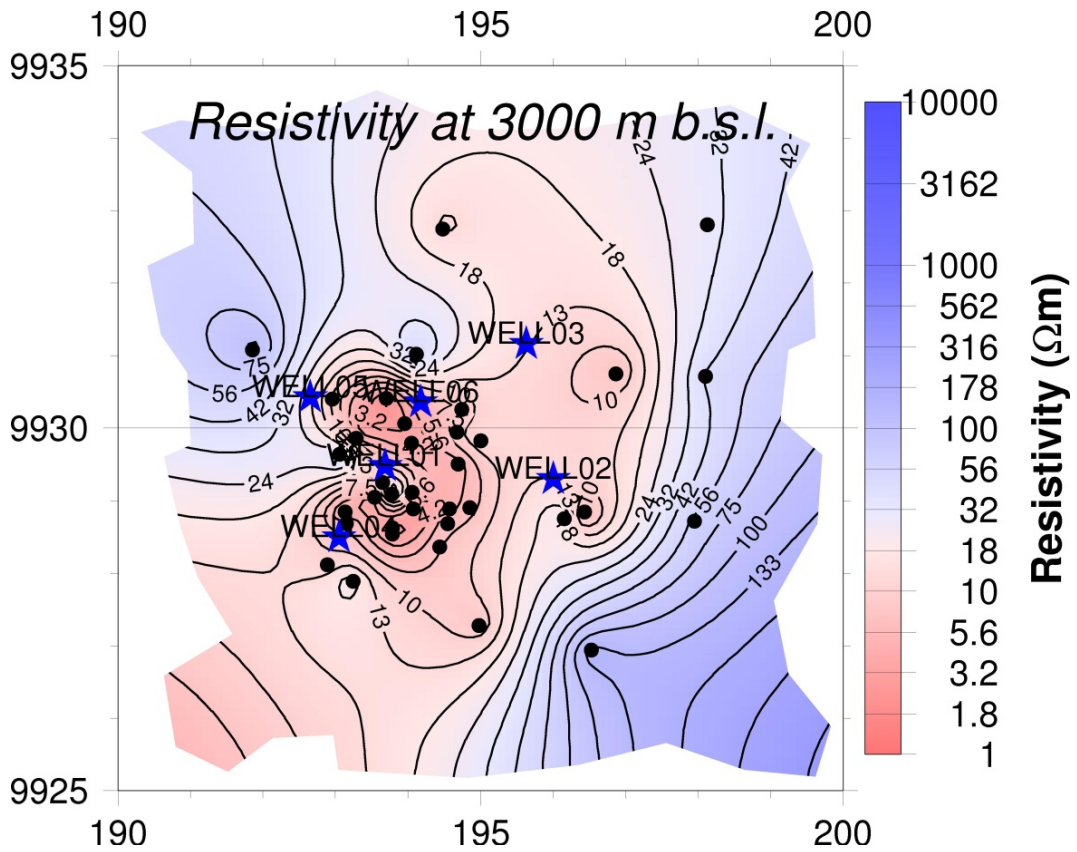


FIGURE 25: Iso-resistivity map at a depth of 3000 m b.s.l.

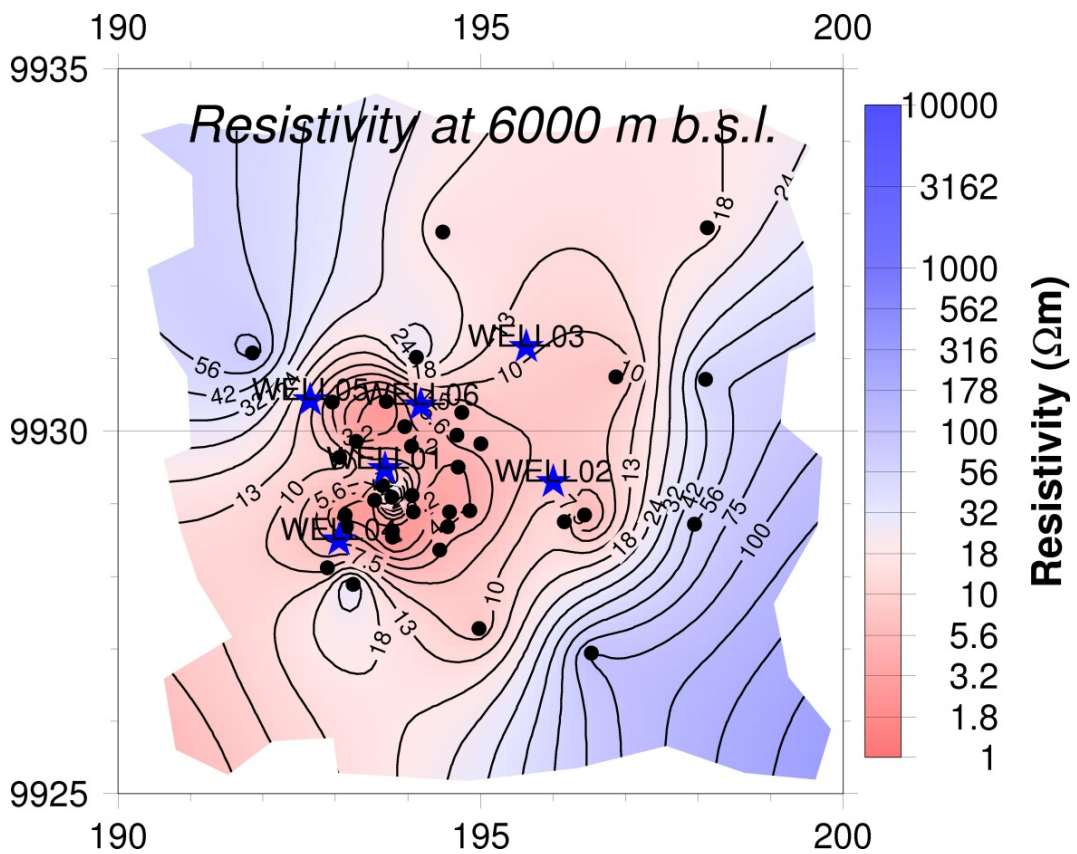


FIGURE 26: Iso-resistivity map at a depth of 6000 m b.s.l.

4.6 Rose diagrams of the electrical strike direction for Eburru

Electrical strike direction gives valuable information about subsurface fractures, and is inferred as showing the pathways for geothermal fluids. Rose diagrams for the electrical strike directions of MT soundings are shown in Figures 27-30 for two different frequency ranges, reflecting different depths. There seems to be a general directional trend of 30 degrees to the East of geographic North. The Tipper confirms this. This can be interpreted such that, in the case of Eburru, at shallow depths there seems to be flow in northeast aligned fractures. At greater depths, the flow seems to be in all directions and this could be due to the effect of the proposed heat source.

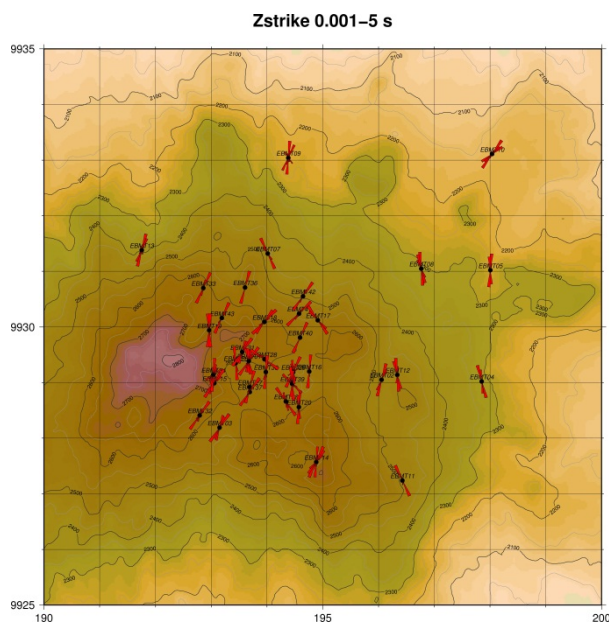


FIGURE 27: Rose diagram of the electrical strike based on Zstrike for periods 0.001-5 s

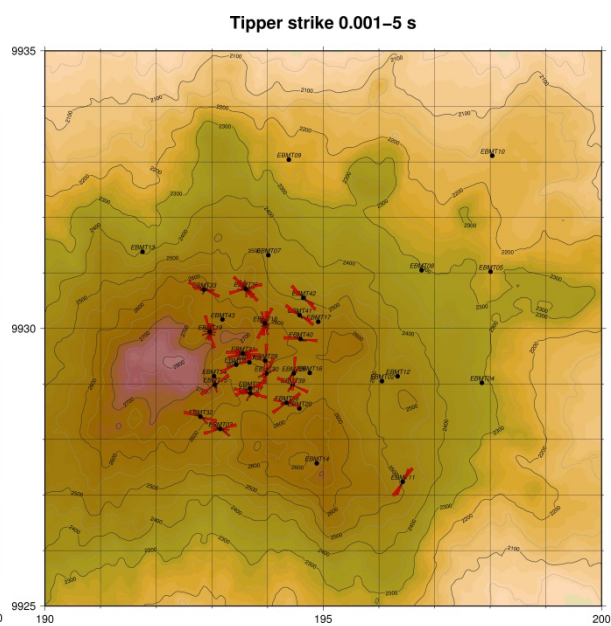


FIGURE 28: Rose diagram of the electrical strike based on Tipper for periods 0.001-5 s

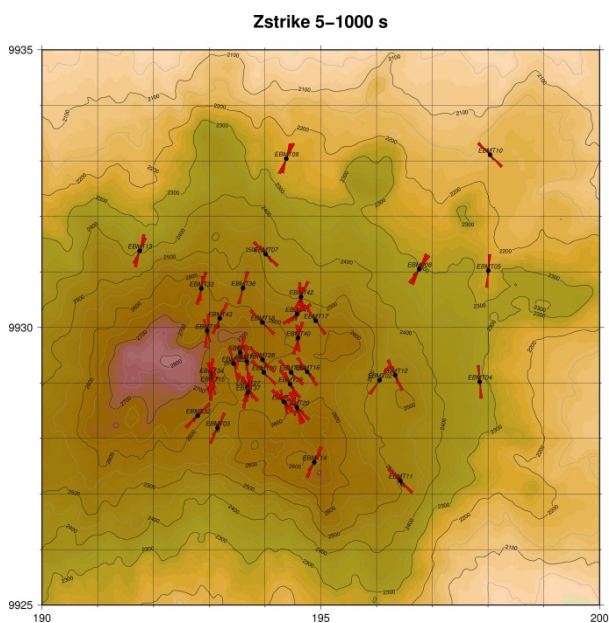


FIGURE 29: Rose diagram of the electrical strike based on Zstrike for periods 5-1000 s

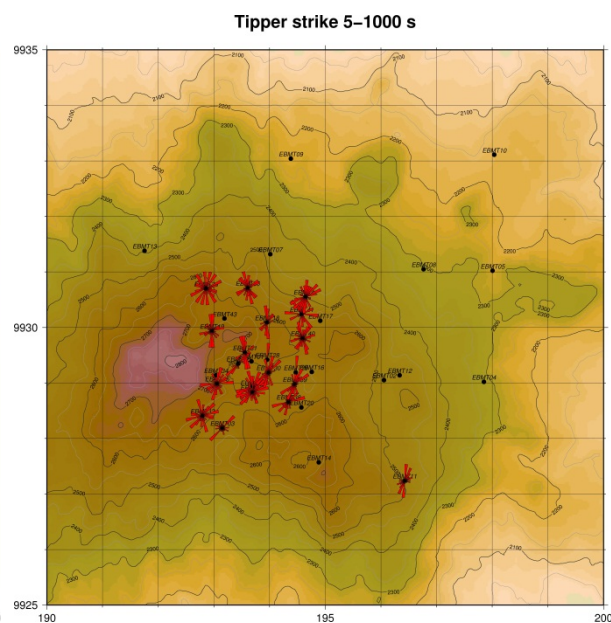


FIGURE 30: Rose diagram of the electrical strike based on Tipper for periods 5-1000 s

4.7 Conclusions

The resistivity cross-sections, based on joint 1D inversion of MT and TEM data, show a geothermal system including three major resistivity bodies. Close to the surface, high resistivity is seen $>70 \Omega\text{m}$ which is interpreted as being due to unaltered rocks. Eburru is home to many geothermal manifestations; and low-resistivity pockets noted close to the surface, about $10 \Omega\text{m}$, are indicative of these surface alterations. These are the conductive clays and low-temperature alteration minerals deposited at the surface. The intermediate zone is a very conductive layer $<10 \Omega\text{m}$, the smectite-zeolite zone. This is the conductive clay cap of the geothermal system. Below this layer, the mixed-layer clay zone and the chlorite epidote-zone are found, indicating alteration temperatures greater than 230°C . Further below, there is a conductive body at great depths which is interpreted as the heat source of the geothermal system. The drillholes in Eburru were used to compare the subsurface resistivity with the alteration temperature. Close correlation was found which indicates that well 1 has temperatures above 270°C .

5. GRAVITY METHOD

The gravity method is a passive geophysical technique that is used to measure differences in the earth's gravitational field, at specific locations, that are caused by lateral density variations. The gravity method measures the acceleration at the earth's surface. To obtain the gravitational acceleration, g , Newton's law of gravitation is used, which describes the force between two masses (M , the mass of the earth, and m , the detection mass) separated by the distance, R , i.e. $F=GMm/R^2$, or $g=GM/R^2$, where G is the gravitational constant. The gravity method is applicable when buried objects have different densities from the surrounding material. However, gravity measured on the earth's surface is affected also by topography, the shape of the earth and its rotation, and tides. These factors must be removed before interpreting gravity data for subsurface features. The final form of the processed gravity data can be used in many types of applications such as for subsidence or uplift, many types of engineering and environmental problems, including determining the thickness of the surface or near-surface soil layer, changes in water table levels, and the detection of buried tunnels, caves, sinkholes and near-surface faults.

The collected gravity data can be presented and applied in different ways. A gravity map showing Bouguer anomalies is used for exploration. Microgravity measurements are used to monitor small changes in gravity associated with mass removal from the geothermal reservoir.

5.1 Gravity corrections

Gravity corrections or reductions are carried out to remove the effects on measured earth's gravitational field in order to reveal the density contrasts of the underlying rocks. Several corrections are applied to reduce the data recorded by the gravimeter. These include latitudinal variations, elevation changes, topographic changes and tides (Keary et al., 2002). But first the following computations are made to calculate the gravity for the stations:

Instrumental calibration: This is either provided by the manufacturer of the gravity meter or obtained by measurements in special calibration lines.

Free-air correction, which is due to the height of the instrument above the ground or marker.

Tidal correction: This effect is a result of the gravitational attractions of the sun and the moon. It must be removed from the gravity readings. This effect can be computed, knowing the time and location of the reading.

Drift correction: The drift of the gravimeter is removed through repeated readings at stations that are observed more than once in the same field trip. A drift curve is plotted against time and assumed to be linear between consecutive readings (Keary et al., 2002).

When a gravity value has been obtained for a site, the following corrections are usually made:

Latitude correction: The earth's gravity field varies significantly with latitude. At the equator, the earth's gravity field is weaker due to the bulge effect as a result of centrifugal force caused by the rotation of the earth (see Figure 31). The gravity measured near the poles is also higher than at the equator because the distance from the centre of the earth to the poles is smaller than the distance to the equator.

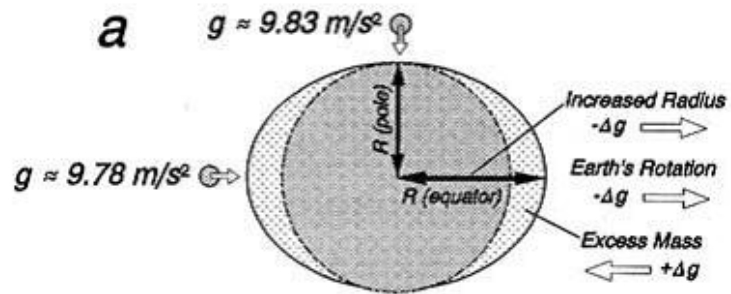


FIGURE 31: Reduced gravity caused by centrifugal acceleration and different distance from the centre of the earth

Elevation corrections:

These corrections include the free air correction, Bouguer correction, and terrain correction.

Free-air anomaly: The free-air gravity anomaly is calculated using the following formula:

$$FA = g_{\text{obs}} - g_N + 3.086 H (\mu\text{ms}^{-2})$$

where g_{obs} = Observed gravity;
 g_N = Normal gravity on the ellipsoid at that latitude;
 H = Height of the station above the geoid (m).

The Bouguer anomaly, BA, is calculated using the following formula:

$$BA = FA - 0.4191 \times 10^{-3} \rho H (\mu\text{ms}^{-2}) + g_T$$

where FA = Free air gravity anomaly
 ρ = Density (kg/m^3)
 g_T = Terrain correction


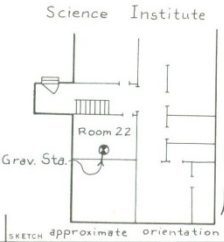
Terrain corrections: Gravity anomalies are calculated by assuming that the gravity station is on a horizontal plane. If the topography differs from this plane, this assumption is not valid and a terrain correction must be applied. Hills above the observation point tend to attract a mass upwards while valleys below the observation point reduce the downward attraction. In both cases, a positive terrain correction must be made. The correction is an integral of the gravitational effect of the mass above or the mass deficit below. The correction depends on the density of the subsurface strata (Murray and Tracey, 2001).

5.2 Microgravity monitoring

Prior to a microgravity survey, a network of benchmarks must be established. The benchmarks should be precisely described, so they can be easily found and identified. Benchmarks as old as 50 years or more are still well preserved in some countries; Iceland is a good example. The descriptions of the benchmarks are preserved so that anyone can access the point. Additionally, a photo with prominent features should be attached, if possible. Information obtained from this description includes: the name of the area, a location map, person and agency who established the point, prominent features in

DESCRIPTION			Station name
Abbr. info.	Abbrev. name	Locality	001B
B	Suswa S	Suswa S	
Type of station	Region		
Gravity base station	Rift Valley		
Type of marker	Engraving on marker		
Established by institution or firm	Establ. year/month	Estab. by	
KenGen	2010	IPM	
Description			
The station is at the Empaash primary school 1.5 km south of Suswa town.			
The station is located at the top of a 1.4 m wide concrete porch at the entrance to the new school building. A church is located 60 m to the north of the school and the old school is 30 m to the south. The station is 11 m from the north wall of the house and 15 m from the south wall. A vertical concrete support post is 0.2 m east of the station. The town Mai Mahiu is situated by road A104 approximately 50 km NNW of Nairobi and 40 km due south of Naivasha. From Mai Mahiu drive 30 km west along the MaiMahiu-Narok Road to the Suswa town. The Empaash primary school is approximately 1.5 km southwest of Suswa and 600 m east of the Narok road.			
This station replaces base station A3.			
N NNA NA ANA A ASA SA SSA (S)			Blocking angle in deg. (if it exceeds ten deg.)
S SSV SV VSV V VNV NV NNV (N)			Max blocking angle < degrees
Photo of station		Map/coord. read unless otherwise stated	
Latitude (approx.)		WGS84	
1°03'43"	Longitude (approx.)	Elevation (approx.)	Described by
	36°19'41"	1650 m	IPM

DESCRIPTION			Station name
Abbr. info.	Abbrev. name	Locality	00A3
	Suswa E	Suswa E	
Type of station	Region		
Gravity base station	Rift Valley		
Type of marker	Engraving on marker		
None	None		
Established by institution or firm	Establ. year/month	Estab. by	
Description			
At road junction just east of the Suswa town.			
The site is an unmarked natural station 25 m south of the MaiMahiu-Narok Road and 7 m to the west of a road leading to a purple painted house 60 m to the southeast of the site. The house is labelled Camp Davis.			
The town Mai Mahiu is situated by road A104 approximately 50 km NNW of Nairobi and 40 km due south of Naivasha. From Mai Mahiu drive 30 km west along the MaiMahiu-Narok Road to the Suswa town.			
This station should be avoided.			
N NNA NA ANA A ASA SA SSA (S)			Blocking angle in deg. (if it exceeds ten deg.)
S SSV SV VSV V VNV NV NNV (N)			Max blocking angle < degrees
Photo of station		Map/coord. read unless otherwise stated	
Latitude (approx.)		WGS84	
1°02'49"	Longitude (approx.)	Elevation (approx.)	Described by
	36°20'10"	1620 m	IPM

COUNTRY	TYPE OF STATION	STATION	GRAVITY VALUE (g)
ICELAND	NATIONAL BASE	5450 REYKJAVIK AA	
LOCATION	TYPE OF MARK	ESTABLISHED BY	GRAVITY VALUE (g)
REYKJAVIK	BRASS DISK	AMS and NEA	982,279.68
LATITUDE	LONGITUDE	DATUM / REFERENCE	ELEV.
64° 08.4' N	21° 57.4' W	AMS 1613 III	10.23 (M)
REMARKS			
Station mark stamped "06 1970 5450" H.I. = 0			
The station is located on gravity bench mark 5450, which is set in the top of the concrete floor of Room 22 in the basement of the Science Institute, University of Iceland, in Reykjavik. The Institute is located near the main University buildings, adjacent to the Hotel Saga. For additional information about this station, contact Gudmundur Palmarsson, National Energy Authority.			
			
DATE OF PHOTO: 24 Sept 68		SKETCH approximate orientation	
Described/Recovered BY: T.H.Nilsen		AGENCY: NEA	
		DATE: Sept 68	



COUNTRY	TYPE OF STATION	STATION	GRAVITY VALUE (g)
ICELAND	NATIONAL BASE	5451 REYKJAVIK B	
LOCATION	TYPE OF MARK	ESTABLISHED BY	GRAVITY VALUE (g)
REYKJAVIK	BRASS DISK	MARTIN 1949	982,273.69
LATITUDE	LONGITUDE	DATUM / REFERENCE	ELEV.
64° 08.6' N	21° 55.6' W	AMS 1613 III	36.84 (M)
REMARKS			
Station mark stamped "06 1970 5451" H.I. = 0			
The station is located on gravity bench mark 5451, which is set in the top of the concrete fundament at ground level and 0.1 meter north of a 1.1 meter high and 0.5x0.5 meter large monolith marking the site of the now vanished observatory erected in 1900. The monolith is 32 meters northeast of the statue of Leifur Eiriksson, which is located 50 meters in front of Hallgrimskirja, the largest church in Reykjavik.			
			
DATE OF PHOTO: Sept. 1973		SKETCH	
Described/Recovered BY: G. Thorbergsson		AGENCY: NEA	
		DATE: Sept. 73	

FIGURE 32: Examples of a description of a gravity station in Kenya and in Iceland; the descriptions should always give as much information as possible; it is recommended that photographs be included to ensure easy recognition of a point

the vicinity, coordinates, approximate gravity value and any important remarks about the station (see Figure 32).

5.3 Instrumentation

There are various gravity meters for recording data available in the market today. Gravity meters are of two categories – either absolute or relative. An absolute gravity meter measures the absolute value of gravity each time it makes a measurement. A relative gravity instrument measures the difference in gravity between successive measurements. A relative instrument is used for most exploration surveys. In general, absolute gravity instruments are far more expensive, much bigger, take much longer to make a high-precision measurement, and usually require more knowledge and skill to use than do relative gravity instruments (Nabighian et al., 2005). For the gravity measurements in Theistareykir, a

Scintrex CG-3M gravimeter was used. This gravimeter is relatively easy to use as it is simplified and also automated. The measurements are made repeatedly and stored in the meter. Readings are downloaded every evening to free the memory space and also to ensure data are backed up. It is important to make repeated readings for each station. By providing consistently repeatable readings, one is more confident that high-quality data are being collected. This means higher productivity may be achieved without sacrificing quality. Gravity data acquisition is a relatively simple task that can be performed by one person. However, two people are usually necessary to determine the location (latitude, longitude and elevation) of the gravity stations. The first consideration is a gravity meter. The accuracy of gravity meters can vary greatly. The reading accuracy of relative gravimeters is about $0.01 \mu\text{ms}^{-2}$.

When carrying out gravity measurements, good care must be taken to protect the gravimeter. It should be transported without shaking it. It is especially important to keep it out of direct sunlight; one must also be alert to the power status of the meter at all times.

5.4 Recording of gravity readings

Gravity is measured for various purposes. Gravity data are very useful in the monitoring of geothermal fields, i.e. the exploitation of the resource in order to determine the effects of exploitation. For this purpose the gravity changes are monitored periodically and comparisons are made to check for changes. For these measurements, a network of permanent stations must be established. The network is dependent on the area coverage of the field under exploitation. The best location for these stations is near a road where access is easy. The site for the benchmark should be checked to make sure that it is stable, not with loose geological formations but rather firm in situ rock to ensure that the only movement that may occur is regional, attributed to regional change.

When doing microgravity monitoring, height changes are monitored and comparisons are made with the measured gravity. In most cases the surveyors carry out precise height measurements and share data with the geophysicist. It is important to note that these two field campaigns should be done almost simultaneously or at least within the same season if they are to be used for comparison. To determine the heights – levelling or navigation system (GPS) should be used.

5.5 Gravity survey in Theistareykir high-temperature field NE-Iceland

5.5.1 Introduction

The main aim for doing gravity work in Theistareykir (Figure 2) was to carry out microgravity measurements for monitoring the field prior to and during exploitation of the resource. The main objective of the microgravity project for this report was to be able to collect good quality data for processing.

The active part of the geothermal area lies in the eastern half of the Theistareykir fissure swarm. The geothermal activity covers an area of nearly 10.5 km^2 ; the most intense activity is on the northwest and northern slopes of Mount Baejarfjall (see Figure 33) and in the pastures extending from there northwards to the western part of Mount Ketilfjall. The thermal area covers nearly 20 km^2 if the old alteration in the western part of the swarm is considered part of the thermal area (Ármansson et al., 1986; Saemundsson, 2007). The bedrock in the area is composed of hyaloclastite ridges formed by subglacial eruptions, interglacial lava flows, and recent lava flows (younger than 10,000 yrs). Almost all rock formations are basaltic in composition, but acidic rocks are found in the western part of the fissure swarm, formed in subglacial eruptions up to the last glacial period (Saemundsson, 2007). Rifting is still active in the fissure swarm (Björnsson et al., 2007). Volcanic activity has been relatively infrequent in the area in recent times. Approximately 14 volcanic eruptions have occurred

in the last 10,000 years, but none in the last 2,500 years. Large earthquakes (up to M: 6.9) occur mainly north of the area in the Tjörnes Fracture Zone, which is a right-lateral transform fault zone (Halldórsson, 2005; Björnsson et al., 2007). The Tjörnes Fracture Zone strikes northwest, crosscutting the north-striking fractures as it enters the fissure swarm some 5 km north of the geothermal area (Ármannsson et al., 2000). The volcanic activity ceases in the fissure swarm as it crosses the Tjörnes Fracture Zone, although its northern part remains seismically active (Ármannsson et al., 1986).

Figure 33 shows the gravity network in the Theistareykir area that was surveyed in August 2011.

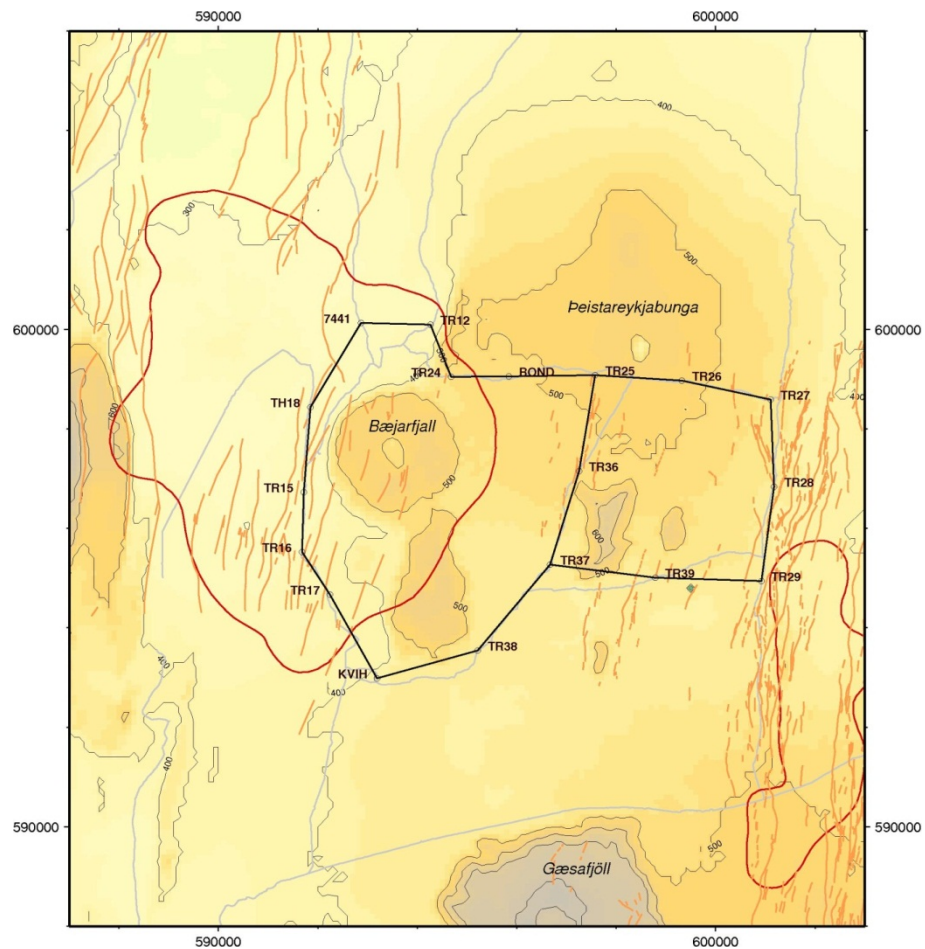


FIGURE 33: The Theistareykir gravity network, surveyed on the 11th and 12th of August 2011

5.5.2 Processing of gravity data

For the processing of the microgravity field data the following series of steps were taken:

1. Convert the readings to mGals (for ScintrexCG-3M the readings are actually in mGals); the calibration is provided by the manufacturer.
2. Add free-air correction to the readings due to the height of the gravimeter above the benchmark.
3. Compute tidal correction for the gravitational effect of the sun and the moon. This correction is based on approximate coordinates of the station and the time of the reading.
4. Use repeated readings to compute and remove drift of the gravimeter during the field trip.
5. Use readings at stations with known gravity values to compute the gravity values at the new unknown stations.

Plotting and ordering of data. About 3-4 readings were recorded for every station. Each reading took about 1 minute and is actually an average of 60 readings, i.e. one reading per second. The raw gravity values were plotted vs. time to detect outliers. The deviation of the readings from the station mean was computed and plotted vs. time.

Correction for the height of the gravimeter above the benchmark. The readings were taken slightly above the bench mark. A free air correction must be done to correct the reading for the height of the meter above the benchmark. The distance from the benchmark to a certain point on the surface of the gravimeter was measured and this length was converted from centimetres to metres and applied to the

free air correction. This correction was added to the gravity reading. If the reading was taken below the benchmark, the correction was subtracted.

Tidal corrections can be computed if the coordinates of a point are known and the time of the day. Figure 34 shows the tidal effect on the 10th and 11th of August 2011. The tidal effect was computed and corrected for. The formula used is the Longman formula (Longman, 1959).

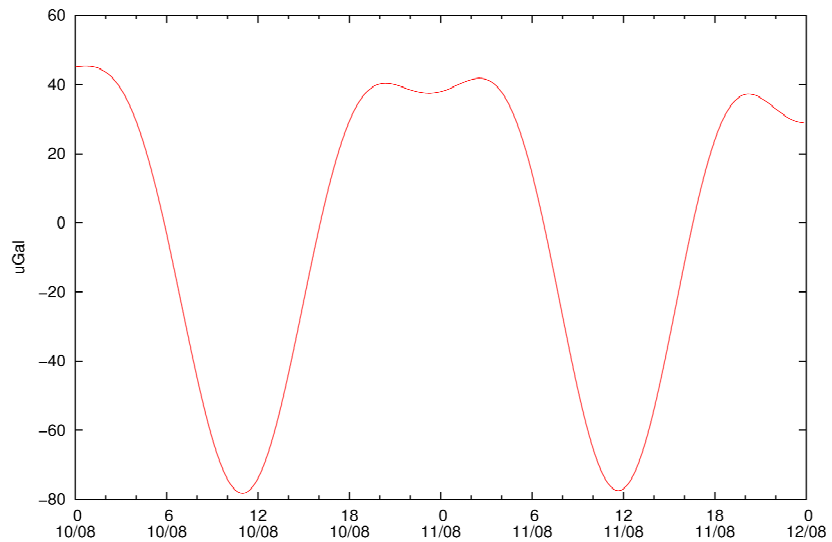


FIGURE 34: Tidal variations in Theistareykir on the 10th to 11th August 2011, the dates of the field work

The drift of the gravity meter

was determined and removed. Before the onset of field work, the gravimeter was set to record every 10 minutes for a period of 48 hours. The tidal effect was removed and a line was fitted to the data by LSQ. The slope of the line was used as an estimate for the drift of the meter during the survey. The remaining drift was removed by using repeated readings. When all the corrections had been performed, a gravity value had been determined for each station.

In the network, each point now had an estimated gravity value. There are points in the network and, thus in the loop, e.g. stations TR38 and TR25, that had more than one estimate. Or put differently, they had redundancy because there were more observations than required. This type of error must be distributed throughout the network, and is commonly known as network adjustment in gravity surveying.

After these corrections, the data are ready for use and can be compared to values from previous surveys to determine the gravity changes. The conceptual model of Theistareykir shows that it is a promising field for exploitation (see Figure 35). When exploitation starts, the changes in gravity as well as the elevation will need to be checked, as the steam is removed from the ground. The resource needs to be monitored during exploitation.

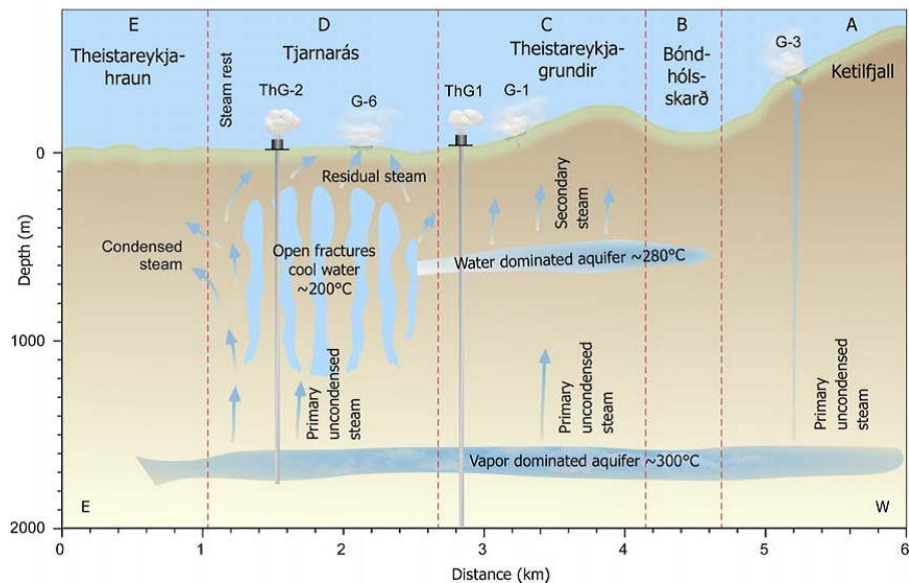


FIGURE 35: The most important aspects of fluid flow in the Theistareykir geothermal system based on surface exploration and results of drilling wells ThG-1 and ThG-2 (Ármannsson, 2009)

5.6 Conclusions

Microgravity surveys require precision in measurements. A good understanding of how to handle the gravimeters is important as these are very delicate equipment. The data obtained from the microgravity surveys need to be checked for consistency and undergo corrections before they can be used for detecting mass changes. Geothermal fields must be monitored to ensure sustainable use of the resource; the data collected can act as a guide for making important decisions such as when to start reinjection to maintain balance. The objective of this study was to collect microgravity data and process it to obtain correct gravity values for the stations. It is important to carry out field surveys alongside precise GPS surveys in order to obtain height measurements if the data is to be used to detect elevation changes due to changes in mass.

7. SUMMARY

The joint 1D inversion of MT and TEM data from Eburru indicates a localized geothermal system around well EW-01. The Eburru geothermal field has many fault lines which are oriented north to south and small craters are distributed around the prospect area. The geothermal system is structurally controlled and seems to be fed by heat from an intrusion. More MT and TEM data need to be collected around the area in order to delineate the extent of the system. TEM and MT data need to be collected at similar stations to enable accurate static correction. Joint inversion is a powerful method used for correcting MT static shift and also for resolving the upper surface using TEM data.

The microgravity method is an inexpensive way to monitor gravity changes around a specific site. This method can be used to check the impacts of exploitation on geothermal resources. To collect gravity data is an art. It requires good field procedures and planning of the survey; the data obtained must be carefully manipulated to produce accurate and reliable results. Theistareykir geothermal field already has an established gravity network set up for taking periodic gravity measurements. In order to draw conclusions from the data set, more data needs to be collected for comparison with previous surveys. The objective of the microgravity project, to become familiarized with field procedures and data reduction, was met.

ACKNOWLEDGEMENTS

I wish to thank the Director, Dr. Ingvar Birgir Fridleifsson, and his Deputy, Mr. Lúdvík S. Georgsson, for the scholarship and the opportunity to come here to Iceland and attend the six months training. In a special way, I would like to thank my supervisors, Mr. Gylfi Páll Hersir and Mr. Knútur Árnason, for their tireless work and the amount of knowledge they have transferred freely to me and my classmates. It has been a wonderful experience, working both in the many field work activities as well as the final projects. I thank you for inspiring me and for always being ready to help. I appreciate Mr. Ingvar Thór Magnússon for guiding me through the field work and gravity project and the long hours spent in working on the programs. Thank you for your patience and help on the project. Thanks also go to the lecturers who have guided us through the specialized and introductory lectures as well as to the staff at ISOR and friends at ISOR and at the UNU. I appreciate Mrs. Ragna for reading through my work and for guidance.

To my classmates, the geophysicists, class wouldn't have been the same without you. It has been a wonderful time working with you; the cooperation we had in class is amazing and I will not forget this. To the other UNU Fellows, you made life interesting and I made a friend of each of you. To my family, my parents, and my friends, you have stood by me through this long period away and you

encouraged me to go on. My dearest friend, Atanasio, thank you for always being so understanding, encouraging me to work hard and for enduring my absence.

Finally, I wish to express my heartfelt gratitude to God for giving me the strength to be able to work on this report.

REFERENCES

- Ármansson, H., 2009: Exploration of the Theistareykir geothermal system, NE-Iceland. *Presented at the "Short Course on Surface Exploration for Geothermal Resources", UNU-GTP and LaGeo, Santa Tecla, El Salvador*, 10 pp.
- Ármansson, H., Gíslason, G., and Torfason, H., 1986: Surface exploration of the Theistareykir high-temperature geothermal area, with special reference to the application of geochemical methods. *Applied Geochemistry*, 1, 47-64.
- Ármansson, H., Kristmannsdóttir, H., Torfason, H., and Ólafsson, M., 2000: Natural changes in unexploited high-temperature geothermal areas in Iceland. *Proceedings of the World Geothermal Congress 2000, Kyushu-Tohoku, Japan*, 521-526.
- Árnason, K., 1989: *Central loop transient electromagnetic sounding over a horizontally layered earth*. Orkustofnun, Reykjavík, report OS-89032/JHD-06, 129 pp.
- Árnason, K., 2006a: *TemX. A graphically interactive program for processing central loop TEM data, a short manual*. ÍSOR – Iceland GeoSurvey, Reykjavík, short manual, 10 pp.
- Árnason, K., 2006b: *TEMTD (program for 1D inversion of central loop TEM and MT data)*. ÍSOR – Iceland GeoSurvey, Reykjavík, short manual, 16 pp.
- Árnason, K., and Karlsdóttir, R., 1996: *Resistivity survey in the Krafla area*. Orkustofnun, Reykjavík, report OS-96005/JHS-03 (in Icelandic), 97 pp.
- Axelsson, G. 2008: Production capacity of geothermal systems. *Presented at the "Workshop for Decision Makers on Direct Heating Use of Geothermal Resources in Asia", UNU-GTP, TBLRREM and TBGMED, in Tianjin, China*, 14 pp.
- Berdichevsky, M.N., and Dmitriev, V.I., 2008: *Models and methods of magnetotellurics*. Moscow State University, Russia, 564 pp.
- Björnsson, A., Saemundsson, K., Sigmundsson, F., Halldórsson, P., Sigbjörnsson, P., and Snaebjörnsson, J.T., 2007: *Geothermal projects in NE-Iceland at Krafla, Bjarnarflag, Gjástykki and Theistareykir; Assessment of geo-hazards affecting energy production and transmission systems emphasizing structural design criteria and mitigation of risk*. Landsvirkjun – National Power Company, report LV-2007/075.
- Castells, A.M., 2006: *A magnetotelluric investigation of geophysical dimensional and study of the central Betic crustal structure*. University of Barcelona, Barcelona, Department of Geodynamics and Geophysics, PhD thesis, 68 pp.
- Flóvenz, Ó.G., Spangenberg, E., Kulenkampff, J., Árnason, K., Karlsdóttir, R. and Huenges E., 2005: The role of electrical conduction in geothermal exploration. *Proceedings of the World Geothermal Congress 2005, Antalya, Turkey*, CD, 9 pp.
- García, X., and Jones, A.G., 2005: A new methodology for the acquisition and processing of audio-magnetotelluric (AMT) data in the AMT dead band. *Geophysics*, 70-5, 119-126.
- Georgsson, L.S., 2009: Geophysical methods in geothermal exploration. *Presented at "Short Course IV on Exploration for Geothermal Resources", UNU-GTP, KenGen, and GDC, Lake Bogoria and Lake Naivasha, Kenya*, 17 pp.

- Halldórsson, P., 2005: *Earthquake activity in North Iceland*. Meteorological Office of Iceland – Vedurstofa Íslands, Reykjavík, report 05021 VÍ-ES-10 (in Icelandic), 39 pp.
- Hersir, G.P., and Árnason, K., 2009: Resistivity of rocks. *Paper presented at the Short Course on Surface Exploration for Geothermal Resources, organized by UNU-GTP and LaGeo, Santa Tecla, El Salvador*, 8 pp.
- Hersir, G.P., and Björnsson, A., 1991: *Geophysical exploration for geothermal resources. Principles and applications*. UNU-GTP, Iceland, report 15, 94 pp.
- Jones, A.G., 1983: The problem of "current channeling": a critical review. *Geophysical Surveys*, 6, 79-122.
- Jones, A.G., 1988: Static shift of magnetotelluric data and its removal in a sedimentary basin environment. *Geophysics*, 53-7, 967-978.
- Keary, P., Brooks, M., and Hill, I., 2002: *An introduction to geophysical exploration*. Blackwell Scientific Publications, Oxford, 262 pp.
- Lagat, J., 2003: Geology and the geothermal systems of the southern segment of the Kenya Rift. *Proceedings of the International Geothermal Conference IGC2003, Multiple integrated uses of geothermal resources, Reykjavik*, S12, 33-40.
- Longman, I.M., 1959: Formulas for computing the tidal acceleration due to the moon and the sun. *J. Geophys. Research*, 64, 2351-2355.
- MacNeill, J.D., 1980: *Applications of transient electromagnetic techniques*. Geonics, Ltd., Canada, technical note TN-7.
- Murray, A.S., and Tracey, R.M., 2001: *Best practice in gravity surveying*. Geoscience Australia, unpublished.
- Mwangi, A.W., 2011: *Appendices to the report "Joint 1D inversion of MT and TEM data from Eburru Kenya and processing of gravity data from Theistareykir, NE-Iceland"*. UNU-GTP, Iceland, report 27, appendices, 64 pp.
- Nabighian, M.N., Ander, M.E., Grauch, V.J.S., Hansen, R.O., LaFehr, T.R., Li, Y., Pearson, W.C., Pierce, J.W., Phillips, J.D., and Ruder, M.E., 2005: The historical development of the gravity method in exploration. *Geophysics*, 70-6, 63-89. Webpage: utam.gg.utah.edu/edhelper/papers/grav.pdf
- Omenda, P.A., and Karingithi, C.W., 1993: Hydrothermal model of Eburru geothermal field, Kenya. *Geothermal Resources Council, Transactions*, 17, 155-160.
- Ouma, P.A., 2010: Geothermal exploration and development of the Olkaria geothermal field. *Paper presented at "Short Course V on Exploration for Geothermal Resources", organized by UNU-GTP, GDC and KenGen, at Lake Bogoria and Lake Naivasha, Kenya*, 16 pp.
- Phoenix Geophysics, 2005: *Data processing user guide*. Phoenix Ltd., users guide.
- Saemundsson, K., 2007: *The geology at Theistareykir*. ÍSOR – Iceland GeoSurvey, Reykjavík, report ISOR-07270 (in Icelandic), 23 pp.
- SEG, 1991: *MT/EMAP data interchange standard*. Society of Exploration Geophysicists, 112 pp.
- University of Washington, 2011: Magnetotelluric research overview. University of Washington, webpage: www.geophys.washington.edu/SolidEarth/Magnetotellurics/overview.html.
- Velador, J.M., Omenda, P.A., and Anthony, E.Y., 2002: Geology and the origin of trachytes and pantellerites from the Eburru volcanic field, Kenya Rift. *Presented at the AGU Fall Meeting 2002*. Webpage: adsabs.harvard.edu/abs/2002AGUFM.V62B1416V.